A fractional K-BKZ constitutive formulation for describing the nonlinear rheology of multiscale complex fluids

Citation: Jaishankar, Aditya, and Gareth H. McKinley. "A Fractional K-BKZ Constitutive Formulation for Describing the Nonlinear Rheology of Multiscale Complex Fluids." J. Rheol. 58, no. 6 (November 2014): 1751–1788.

As Published: http://dx.doi.org/10.1122/1.4892114

Publisher: American Institute of Physics (AIP)

Persistent URL: http://hdl.handle.net/1721.1/97686

Version: Author's final manuscript: final author's manuscript post peer review, without publisher's formatting or copy editing

A Fractional K-BKZ Constitutive Formulation for Describing the Nonlinear Rheology of Multiscale Complex Fluids

Aditya Jaishankar[1] and Gareth H. McKinley[1, a)]

Department of Mechanical Engineering, Massachusetts Institute of Technology, Cambridge, MA 02139, USA

(Dated: 13 June 2014)

The relaxation processes of a wide variety of soft materials frequently contain one or more broad regions of power-law–like or stretched exponential relaxation in time and frequency. Fractional constitutive equations have been shown to be excellent models for capturing the linear viscoelastic behavior of such materials, and their relaxation modulus can be quantitatively described very generally in terms of a Mittag-Leffler function. However, these fractional constitutive models cannot describe the nonlinear behavior of such power-law materials. We use the example of Xanthan gum to show how predictions of non-linear viscometric properties such as shear-thinning in the viscosity and in the first normal stress coefficient can be quantitatively described in terms a nonlinear fractional constitutive model. We adopt an integral K-BKZ framework and suitably modify it for power-law materials exhibiting Mittag-Leffler type relaxation dynamics at small strains. Only one additional parameter is needed to predict nonlinear rheology, which is introduced through an experimentally measured damping function. Empirical rules such as the Cox-Merz rule and Gleissle mirror relations are frequently used to estimate the nonlinear response of complex fluids from linear rheological data. We use the fractional model framework to assess the performance of such heuristic rules and quantify the systematic offsets, or shift factors, that can be observed between experimental data and the predicted nonlinear response. We also demonstrate how an appropriate choice of fractional constitutive model and damping function results in a nonlinear viscoelastic constitutive model that predicts a flow curve identical to the elastic Herschel-Bulkley model. This new constitutive equation satisfies the Rutgers-Delaware rule. that is appropriate for yielding materials. This K-BKZ framework can be used to generate canonical three-element mechanical models that provide nonlinear viscoelastic generalizations of other empirical inelastic models such as the Cross model. In addition to describing nonlinear viscometric responses, we are also able to provide accurate expressions for the linear viscoelastic behavior of complex materials that exhibit strongly shear-thinning Cross-type or Carreau-type flow curve. The findings in this work provide a coherent and quantitative way of translating between the linear and nonlinear rheology of multiscale materials, using a constitutive modeling approach that involves only a few material parameters.

Keywords: power-law, Cox-Merz, Gleissle mirror relations, Fractional Maxwell Model, Springpot, K-BKZ, Damping Function, Rutgers-Delaware rule

[a)]Electronic mail: gareth@mit.edu

I. INTRODUCTION

Many complex fluids and soft solids are characterized by the presence of a very broad range of microstructural length and time scales. Examples of such materials include crosslinked polymer networks (Winter and Mours (1997)), microgel dispersions (Ketz, Prud'homme, and Graessley (1988)), foams (Khan, Schnepper, and Armstrong (1988)), colloidal suspensions (Mason and Weitz (1995); Rich, McKinley, and Doyle (2011)) and soft glassy materials (Sollich (1998)). Such materials are commonly used to formulate consumer products such as foods (Ng and Mckinley (2008); Gallegos, Franco, and Partal (2004)), in biological materials (Fabry *et al.* (2001)) and in nanocomposite materials (Krishnamoorti and Giannelis (1997)). One common characteristic of these materials is the presence of broad power-law spectra during stress relaxation or small amplitude oscillatory tests due the multiscale nature of their microstructure. In fact Boltzmann considered menory functions of the form $G(t) \sim 1/t$ in his original work on linear viscoelasticity (Markovitz (1977)). The mechanical models that are commonly used to describe the rheology of multiscale materials often require the introduction of a large number of fitting parameters and are thus unsatisfactory. Blair, Veinoglou, and Caffyn (1947a) have argued that describing the rheological response of these materials in terms of conventional material properties such as coefficients of viscosity and elastic moduli that characterize each possible relaxation mode is far from ideal as it requires a very large number of parameters. They suggest that *quasi-properties*, which are intermediate quantities between a viscosity and a modulus (units: Pa s^{α}, $0 < \alpha < 1$) offer a compact mathematical framework to describe such materials with complex multiscale microstructures.

In the linear regime, fractional constitutive equations have been shown to be particularly good models to describe such materials (Schiessel *et al.* (1995); Bagley and Torvik (1983b); Nonnenmacher (1991); Glockle and Nonnenmacher (1991); Metzler *et al.* (1995)) and naturally introduce material parameters that describe these quasi-properties. For example, Bagley and Torvik (1983a) show that the high frequency response of the Rouse model has an equivalent fractional constitutive representation. Fractional constitutive models utilize a rheological element known as the springpot (Koeller (1984); Jaishankar and McKinley (2013)), that interpolates between the responses of a spring and a dashpot, using the mathematical definition of a fractional derivative. Textbooks such as those by Podlubny (1999), Oldham

and Spanier (1974), Mainardi (2010) and Miller and Ross (1993) are excellent references for a background on the mathematics of these derivatives. Each springpot is characterized by two parameters: a quasi-property generically denoted $\mathbb{V}$ and a fractional exponent α. The physical basis for fractional constitutive models is found in the fact that multiscale systems often display anomalous sub-diffusion on the microscopic scale, and the root mean square distance of passive tracers $\langle \Delta x^2 \rangle$ scales with time as $\langle \Delta x^2 \rangle \sim t^\alpha$, $0 < \alpha < 1$ (Metzler, Barkai, and Klafter (1999); Metzler and Klafter (2000); Sokolov, Klafter, and Blumen (2002a); Sharma and Cherayil (2010)). Using the fractional Fokker-Plank equation (Sokolov, Klafter, and Blumen (2002b)) in conjunction with the generalized Stokes-Einstein equation (Mason (2000)) it can be shown how the sub-diffusive behavior seen in microrheology experiments arises from the multiscale microstructure of these materials, and also leads to power-law stress relaxation observed in bulk rheology experiments. Muthukumar (1985) has argued that power-law materials such as branched polymers, percolation clusters and aggregates can be idealized as having non-integer or *fractal* dimensions.

Many multiscale materials typically exhibit a broad power-law regime of stress relaxation over many decades of timescales, but at sufficiently long times (or low frequencies) ultimately transition into either a sol-like flow regime or a gel-like plateau regime. Both of these responses can be captured by appropriate two element fractional constitutive models arranged in series or parallel. The Fractional Maxwell Model (FMM) consists of two springpot elements in series (Friedrich and Braun (1992)). The FMM compactly describes the rheological properties of multiscale materials that exhibit sol-like flow at long timescales. In a previous publication, we have shown using the example of viscoelastic interfaces formed from globular protein solutions that the FMM can quantitatively predict the *linear* rheological behavior of complex fluids under a range of different deformation conditions (Jaishankar and McKinley (2013)). The relaxation modulus in the FMM takes the analytical form of a Mittag-Leffler function, which exhibits stretched exponential (KWW) behavior at short times, and power-law behavior at long timescales (Metzler and Klafter (2002)).

On the other hand, complex fluids exhibiting a gel-like response in the long time scale limit are better modeled by the Fractional Kelvin-Voigt Model (FKVM). This second canonical fractional constitutive equation comprises of two springpots arranged in parallel. Both the FMM as well as the FKVM are characterized by only four parameters — two power-law exponents, which control the scaling for the temporal and frequency response, and two

quasi-properties, which set the scales for magnitude of the stresses in these multiscale materials. Examples of the successful application of these two canonical fractional models to describe the linear rheology of complex multiscale materials include red blood cell membranes (Craiem and Magin (2010)), smooth muscle cells (Djordjević *et al.* (2003)), food gums (Ma and Barbosa-Canovas (1996)) and comb-shaped polymers (Friedrich (1992)). However we note that while the linear viscoelastic predictions of fractional models have now been extensively studied, there is an absence of fractional constitutive equations that are able to predict the *nonlinear* rheological response of these complex materials observed at large strain. Yang, Lam, and Zhu (2010) provide an overview of previous attempts at developing appropriate frame invariant models utilizing fractional derivatives and also list their shortcomings. They develop an appropriate finite strain measure coupled with the Mittag-Leffler relaxation kernel, and this leads to a frame-invariant Fractional Upper Convected Maxwell formulation. However, this model suffers from the same limitations of all quasi-linear models (Bird, Armstrong, and Hassager (1987)) and is unable to predict shear-thinning in the viscosity, and also predicts a constant first normal stress coefficient Ψ_1 at all shear rates. This absence of shear-thinning effects is in stark contrast to the very broad shear-thinning response observed in common complex multiscale materials such as Xanthan gum.

Larson (1985) has previously shown that by using the integral form of the K-BKZ type equation with a simple power-law relaxation kernel and a suitable strain dependent damping function, the nonlinear rheology of polydisperse polymer melts can be accurately predicted. However as we have noted above, a single power-law type relaxation kernel of the form $G(t) = ct^{-\alpha}$, in which c and $0 < \alpha < 1$ are the only material constants that characterize the linear response, does not adequately characterize the viscoelastic response of many complex materials that show two or more distinct power-law regimes during relaxation. One commonly employed experimental technique for gaining insight into nonlinear rheological properties of complex materials is through the use of empirical rules such as the Cox-Merz rule (Cox and Merz (1958)), Laun's rule (Laun (1986)) or the Gleissle Mirror Relations (Leblans, Sampers, and Booij (1985); Bird, Armstrong, and Hassager (1987)). These empirical rules connect the progressive shear-thinning behavior observed in many complex multiscale materials to the very broad relaxation spectra observed in linear viscoelastic tests such as small amplitude oscillatory shear flow (Bird, Armstrong, and Hassager (1987); Sharma and McKinley (2012)). Booij and Leblans (1983) have shown that irrespective of the particular

form of the relaxation spectrum, viscoelastic materials will obey the Cox-Merz rule when the shear component of the nonlinear strain measure $S_{12}(\dot{\gamma}s)$ satisfies

$$S_{12}(\dot{\gamma}s) = \int_0^{\dot{\gamma}s} J_0(v)\ dv \tag{1}$$

in which $J_0(v)$ is the zeroth order Bessel function of the first kind and $\dot{\gamma}s$ is the total shear strain accumulated in the time interval s. However, Renardy (1997) notes that this relation is not plausible; he demonstrates very generally that materials with a very broad spectrum of relaxation modes, and the simplest possible strain-dependent damping function, do indeed obey rules like the Cox-Merz rule to within *a constant factor*. This assumption of a broad spectrum of relaxation times holds true for a power-law material and we should thus expect that a suitable nonlinear generalization of fractional viscoelastic models can be used to understand the predictive capabilities of these empirical rheological rules.

In this work, we use the K-BKZ framework together with Scott Blair's ideas of quasi-properties and the fractional calculus to quantify the magnitude of this offset factor in the Cox-Merz rule and interpret its existence in terms of the accumulated damage in a multiscale material arising from the nonlinear response to the applied deformation. In Fig. 1 we present a flowchart of the various pathways discussed in this paper to predict nonlinear material response, including the application of the empirically based Cox-Merz rule and the Gleissle mirror relations. We discuss these relationships in more detail in Section IV. We also demonstrate using our K-BKZ model how one may quantify the systematic offset that is commonly observed between these empirical relationships and experimentally measured data.

We begin with the Fractional Maxwell Model (Jaishankar and McKinley (2013)) and extend Larson's K-BKZ approach to include relaxation kernels of Mittag-Leffler type. Incorporating Renardy's arguments for broad relaxation spectra, we show that by using an appropriate damping function that accurately captures the transition to nonlinear shear-thinning behavior, one can make accurate predictions of both steady shear viscosity $\eta(\dot{\gamma})$ as well as first normal stress coefficient $\Psi_1(\dot{\gamma})$ as a function of shear rate. To demonstrate the quantitative capabilities of the model, we compare our predictions with nonlinear rheological data obtained for Xanthan gum, a complex semi-rigid, branched and physically associated

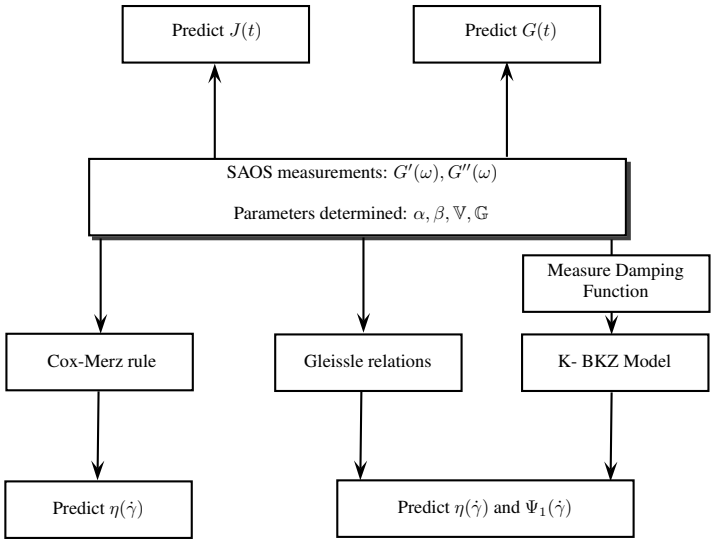

FIG. 1. Flowchart showing the pathways described in this paper to arrive at viscometric material functions for multiscale materials. Beginning with a simple linear viscoelastic experiment such as Small Amplitude Oscillatory Shear (SAOS), and characterizing the power-law responses of the material using a fractional constitutive model, we can make accurate predictions of other linear material functions such as the creep compliance $J(t)$ and the relaxation modulus $G(t)$. We also show in this paper that by measuring the damping function $h(\gamma)$ and using a K-BKZ framework in conjunction with the previously determined quasi-properties, nonlinear material functions such as the steady shear viscosity $\eta(\dot{\gamma})$ and the first normal stress coefficient $\Psi_1(\dot{\gamma})$ can be evaluated accurately.

polysaccharide that shows a very broad relaxation spectrum. Empirical rules such as the Cox-Merz rule and the Gleissle Mirror relations (cf. Fig. 1) have been reported to over-predict the nonlinear material functions in the case of polysaccharide gums (Oertel and Kulicke (1991); Ross-Murphy (1995)) and we show that this over-prediction is connected directly to the power-law exponents that characterize the shape of the material's relaxation spectrum.

Another rule relating steady shear flow and oscillatory flow, referred to by Krieger (1992) as the Rutgers-Delaware rule, has been proposed by Doraiswamy *et al.* (1991) for materials in which the timescale of the applied deformation is much shorter than a characteristic structural recovery time. This is often the case with complex materials that yield upon the application of a small deformation. These materials appear gel-like or solid-like at rest and yield or flow at large strains. We use the Fractional Kelvin-Voigt Model (FKVM) that characterize the linear viscoelastic properties of solid-like power-law gels, along with a damping function proposed by Tanner and Simmons (1967) to derive the Herschel-Bulkley

equation for flow of a yielding material under steady shear. For this nonlinear fractional gel, we also demonstrate that we can recreate exactly the Rutgers-Delaware rule proposed by Doraiswamy *et al.* (1991).

The remainder of this paper is organized as follows: in the next section we present details of the preparation of the Xanthan gum solutions used in this study as prototypical power-law materials. The linear viscoelastic properties of these gums can be well characterized in compact form using the concept of quasi-properties and fractional constitutive equations. We also discuss in this section the experimental protocol and instrumentation employed for rheometric measurements. In the third section, we briefly review some of the mathematical preliminaries of fractional calculus and springpots. The fourth section presents our experimental results and theoretical insights from the K-BKZ framework, the quantification of the shift factors that exist in the predictions of empirical relationships such as the Cox-Merz rule and the development of the Herschel-Bulkley model for yielding multiscale materials. We also derive exactly the Rutgers-Delaware rule for such materials. We next discuss the Fractional Zener Model (FZM) and show how this leads to a prediction of the flow curves of materials that are well described by the familiar inelastic Cross and Carreau models. The advantage of our approach is that in addition to the correct nonlinear flow curves, we are also able to obtain expressions for the linear viscoelastic response of materials described by the Herschel-Bulkley and Cross models. Furthermore, we also obtain predictions for the first normal stress coefficient $\Psi_1(\dot{\gamma})$ for such materials.

II. MATERIALS AND METHODS

Xanthan is a highly branched high molecular weight polysaccharide produced by the *Xanthomonas campestris* bacterium (Rees and Welsh (1977); Lapasin and Pricl (1995)). Both the molecular structure as well as the rheology of Xanthan gum has been extensively characterized by Cuvelier and Launay (1986), Whitcomb and Macosko (1978), Rochefort and Middleman (1987), Ross-Murphy, Morris, and Morris (1983) and Tako (1992), amongst others. The Xanthan gum used in this study was sourced from Sigma-Aldrich (SKU: G1253) in powder form. To prepare the solutions, the specified amount of the powder was weighed using a Mettler-Toledo weighing scale (resolution 10^{-4} g) and added to deionized water at 25°C to prepare a stock solution of 1 wt.% Xanthan gum solution. The mixture was then

stirred using a magnetic stirrer for 24 hours at 300 rpm. To enable complete biopolymer hydration, the solution was stored at 4°C for at least another 12 hours before being used for rheological testing (Sanchez *et al.* (2002)). Additional solutions of 0.5 wt.% and 0.25 wt.% were prepared by careful dilution of the 1 wt.% stock solution immediately after the initial 24 hour stirring, and were also allowed to hydrate at 4°C for 12 hours.

The rheometry performed in this study was carried out using a stress controlled DHR-3 rheometer (TA Instruments, Newcastle, DE) with a 6 cm diameter 2° cone-and-plate fixture. Care was taken to prevent evaporation by saturating the environment around the test fluid using a solvent trap. All experiments were performed on a Peltier plate at a constant temperature of 25°C.

III. MATHEMATICAL PRELIMINARIES

The Caputo definition for the fractional differentiation to order $0 < \alpha < 1$ of a function $\gamma(t)$ is given in terms of an integro-differentiation operation as (Caputo (1967); Surguladze (2002))

$$\frac{d^{\alpha}\gamma(t)}{dt^{\alpha}} = \frac{1}{\Gamma(1-\alpha)} \int_{0}^{t} (t-t')^{-\alpha} \dot{\gamma}(t') \, dt' \tag{2}$$

where $\dot{\gamma}(t) = d\gamma(t)/dt$ indicates conventional first order differentiation with respect to time. Other definitions for the fractional derivative exist, such as the Riemann-Liouville definition; however the Caputo derivative and the Riemann-Liouville derivatives can be shown to be equivalent if the function being differentiated (in this case $\gamma(t)$) has n continuous derivatives all of which tend to 0 as $t \to \infty$, where $n - 1 < \alpha < n$. The Caputo definition is a more convenient formulation for rheological applications due to the relative ease of implementing initial conditions (Heymans and Podlubny (2005)). Therefore, we will use the Caputo definition of the fractional derivative in this paper. springpot (Koeller (1984); Torvik and Bagley (1984)) as being written in the form

$$\sigma(t) = \mathbb{V}\frac{d^{\alpha}\gamma(t)}{dt^{\alpha}} = \frac{\mathbb{V}}{\Gamma(1-\alpha)} \int_{0}^{t} (t-t')^{-\alpha} \dot{\gamma}(t') \, dt' \tag{3}$$

in which $\sigma(t)$ is the instantaneous stress in the element and $\gamma(t)$ is the instantaneous strain. The quantity $\mathbb{V}$ is best referred to as a quasi-property (Blair, Veinoglou, and Caffyn (1947a); Jaishankar and McKinley (2013)) with units of Pa s^{α} and is a measure of the underlying relaxation processes occurring in a multiscale material rather than a material property itself. In the limits of $\alpha = 0$ and $\alpha = 1$ we retrieve the constitutive equations of a Hookean spring and a Newtonian dashpot respectively (for $\alpha = 1$, the Caputo definition for the fractional derivative given in Eq. (2) is different; see, for example, Surguladze (2002) for details). Because $0 \leq \alpha \leq 1$ for a springpot, this fractional constitutive element interpolates between the ideal limits of spring and dashpot, and the quasi-property $\mathbb{V}$ provides a measure of the magnitude of the stresses arising in a power-law–like material during deformation. A schematic representation of the springpot is shown in Fig. 2a. We note the similarity between Eq. (3) and the Boltzmann superposition integral; in fact, it can rigorously be proved (Koeller (1984)) that the relaxation modulus of a single springpot is given by

$$G(t) = \frac{\mathbb{V}t^{-\alpha}}{\Gamma(1-\alpha)} \tag{4}$$

Because the constitutive equation of a springpot as embodied in Eq. (3) involves a linear superposition integral, the techniques of Laplace and Fourier transforms may be applied to fractional derivatives, and this enables us to derive expressions for standard linear viscoelastic material functions such as the relaxation modulus $G(t)$ as well as the storage and loss moduli, $G'(\omega)$ and $G''(\omega)$, respectively. Mathematical details of these transforms as applied to fractional derivatives may be found in standard textbooks (Miller and Ross (1993); Podlubny (1999); Friedrich, Schiessel, and Blumen (1999)). Valério *et al.* (2013) have recently published a comprehensive table of formulas pertaining to various mathematical operations on fractional derivatives.

Previous experiments performed on Xanthan gum have documented the very broad relaxation spectra in this complex hydrocolloid with power-law like regimes due to branching and physical associations such as the interchain hydrogen bonds that continuously break and reform. We use the Fractional Maxwell Model (FMM) to model the linear viscoelasticity of Xanthan gum solutions in a compact form. This model consists of two springpots connected in series, as shown schematically in Fig. 2b. The constitutive equation for this fractional

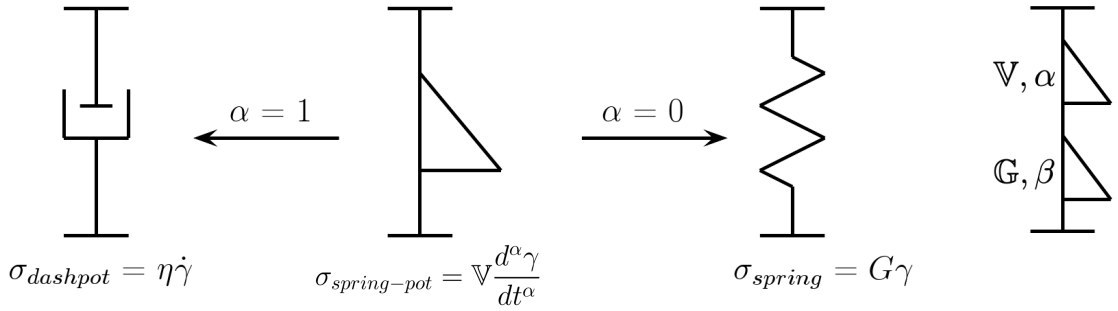

(a) (b)

FIG. 2. (a) Schematic figure of a springpot characterized by a power-law exponent α and a quasi-property $\mathbb{V}$ with dimensions Pa s^{α}. In the limits of $\alpha = 1$ and $\alpha = 0$, the springpot reduces to a Newtonian dashpot with viscosity η and Hookean spring of modulus G respectively. The corresponding linear viscoelastic constitutive equations are given below each element. (b) Schematic figure of the Fractional Maxwell Model (FMM), showing two springpots in series. Each springpot in this four parameter model is characterized by two parameters; a quasi-property ($\mathbb{V}$ or $\mathbb{G}$) and a fractional exponent (α or β).

constitutive model is given by (Jaishankar and McKinley (2013))

$$\sigma(t) + \frac{\mathbb{V}}{\mathbb{G}} \frac{d^{\alpha-\beta}}{dt^{\alpha-\beta}} \sigma(t) = \mathbb{V} \frac{d^{\alpha}\gamma(t)}{dt^{\alpha}} \tag{5}$$

In the above equation, we assume $0 \leq \beta < \alpha \leq 1$ without loss of generality. It has been shown that this model is consistent with the principles of thermodynamics and results in a non-negative internal work and a non-negative rate of energy dissipation. See for example Friedrich (1991) and Lion (1997). We can take the Fourier transform of Eq. (5) to obtain the elastic and loss moduli $G'(\omega)$ and $G''(\omega)$ for the Fractional Maxwell Model respectively as

$$G'(\omega) = \frac{(\mathbb{G}\omega^{\beta})^2 \mathbb{V}\omega^{\alpha} \cos(\pi\alpha/2) + (\mathbb{V}\omega^{\alpha})^2 \mathbb{G}\omega^{\beta} \cos(\pi\beta/2)}{(\mathbb{V}\omega^{\alpha})^2 + (\mathbb{G}\omega^{\beta})^2 + 2\mathbb{V}\omega^{\alpha}\mathbb{G}\omega^{\beta} \cos(\pi(\alpha-\beta)/2)} \tag{6}$$

$$G''(\omega) = \frac{(\mathbb{G}\omega^{\beta})^2 \mathbb{V}\omega^{\alpha} \sin(\pi\alpha/2) + (\mathbb{V}\omega^{\alpha})^2 \mathbb{G}\omega^{\beta} \sin(\pi\beta/2)}{(\mathbb{V}\omega^{\alpha})^2 + (\mathbb{G}\omega^{\beta})^2 + 2\mathbb{V}\omega^{\alpha}\mathbb{G}\omega^{\beta} \cos(\pi(\alpha-\beta)/2)} \tag{7}$$

The corresponding relaxation modulus $G(t)$ for the FMM can be obtained by substituting a step strain $\gamma(t) = \gamma_0 H(t)$ into Eq. (5) solving for $G(t) = \sigma(t)/\gamma_0$. An analytical solution for $G(t)$ can be derived by taking the Laplace transform of the resulting equation, simplifying

and inverting the transform, and we obtain (Schiessel *et al.* (1995))

$$G(t) = \mathbb{G}t^{-\beta}E_{\alpha-\beta,1-\beta}\left(-\frac{\mathbb{G}}{\mathbb{V}}t^{\alpha-\beta}\right) \tag{8}$$

Here $E_{a,b}(z)$ is the generalized Mittag-Leffler function (MLF) defined as (Podlubny (1999))

$$E_{a,b}(z) = \sum_{k=0}^{\infty}\frac{z^k}{\Gamma(ak+b)} \tag{9}$$

We note that setting $\alpha = 1$ and $\beta = 0$ in Eq. (5) yields the linear Maxwell model (a dashpot and a spring in series) and we thus obtain single mode Maxwell-Debye response. Equivalently, setting $\alpha = 1$ and $\beta = 0$ in Eq. (8) also leads to Maxwell-Debye response and the Mittag-Leffler function reduces to simple exponential decay in this limit. Mittag-Leffler type relaxation of the form shown in Eq. (8) for $0 < \beta < \alpha < 1$ results in a broad range of relaxation timescales and more accurately describes the relaxation dynamics of many polymeric systems (Friedrich, Schiessel, and Blumen (1999)) as well as other soft materials, including the Xanthan gums described in this paper. It can be shown using asymptotic expansions of Eq. (8) (Podlubny (1999)) that at short times, $G(t) \approx \mathbb{G}t^{-\beta}/\Gamma(1-\beta)$ and at long times $G(t) \approx \mathbb{V}t^{-\alpha}/\Gamma(1-\alpha)$. Hence this model is very well suited to describe materials displaying two distinct power-law regimes during relaxation. The transition from one power-law to the other occurs when the argument in the MLF function $E_{a,b}(-z)$ is $z \sim \mathcal{O}(1)$. This leads to the identification of a single characteristic time scale in this four parameter model given by $\tau \approx (\mathbb{V}/\mathbb{G})^{1/(\alpha-\beta)}$.

IV. RESULTS AND DISCUSSION

A. Linear Viscoelasticity

In Fig. 3 we show the results of a frequency sweep experiment using small amplitude oscillatory shear (SAOS) on 0.25 wt.% and 0.5 wt.% Xanthan gum. The strain amplitude chosen was $\gamma_0 = 1\%$, and this amplitude was chosen from an independently performed strain amplitude sweep (not shown) to ensure tests are in the linear regime . We note that there are two distinct power-law regimes visible at low and high frequencies respectively, and there is a

gradual transition from one asymptote to the other. The solid and dashed lines represent fits of the data to the predictions for $G'(\omega)$ and $G''(\omega)$ (Eqs. (6) and (7) respectively) obtained from the FMM. We also performed additional SAOS experiments on a 1 wt.% Xanthan gum solution (not shown in Fig. 3 for clarity) which are equally well described by the FMM. The values of the exponents α, β and the quasi-properties $\mathbb{V}, \mathbb{G}$ obtained from these fits are tabulated in Tab. I.

As the concentration of Xanthan gum is increased, the values of α and β progressively decrease, indicating transition to more gel-like behavior, with an increasingly broad spectrum of relaxation times. At the same time, an increase in Xanthan concentration leads to an increase in the quasi-properties $\mathbb{V}$ and $\mathbb{G}$, implying that the magnitude of the stress increases. These constitutive parameters completely characterize the linear rheology of these viscoelastic Xanthan gum solutions and will be used to make predictions of the material response in other deformations. There exists a characteristic frequency at which the two power-law regimes transition from one to the other, and this is determined by the frequency ω_c at which $G'(\omega)$ and $G''(\omega)$ intersect. This can be found by equating Eqs. (6) and (7) and

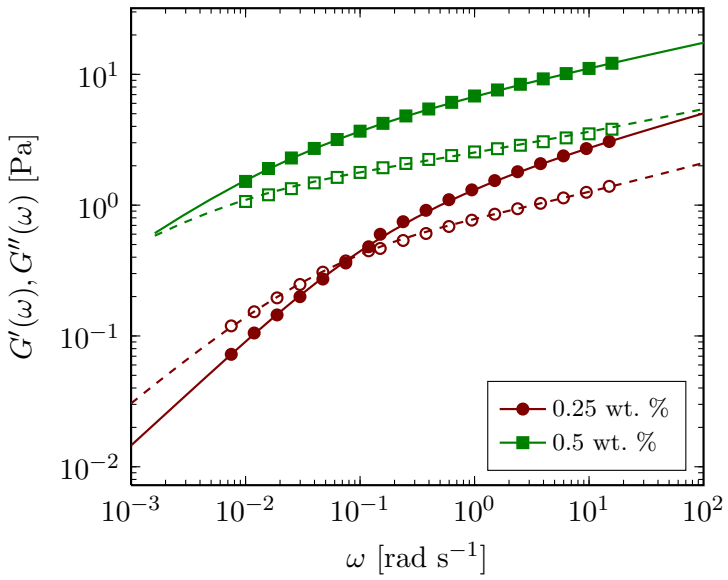

FIG. 3. Small Amplitude Oscillatory Shear (SAOS) experiments performed on different concentrations of Xanthan gum. Data are shown by filled symbols (storage modulus) and hollow symbols (loss modulus) ,while the solid lines are fits to the storage modulus $G'(\omega)$ (Eq. (6)) and the dashed lines are fits to the loss modulus $G''(\omega)$ (Eq. (7)). The parameter values determined for each fluid are given in Tab. I.

TABLE I. Values of the model parameters $\alpha, \beta, \mathbb{V}$ and $\mathbb{G}$ of the FMM for different concentrations of Xanthan Gum.

Conc. [wt. %]	α	β	$\mathbb{V}$ [Pa s$^{\alpha}$]	$\mathbb{G}$ [Pa s$^{\beta}$]	ω_c [rad s^{-1}]	τ [s]
0.25	0.76	0.24	7.02	1.82	7.46×10^{-3}	13.41
0.50	0.64	0.19	71.65	7.82	1.34×10^{-3}	748.74
1.0	0.60	0.14	208.54	22.46	5.4×10^{-4}	1846.05

solving for the crossover frequency:

$$\omega_c = \left(\frac{\mathbb{G}}{\mathbb{V}} \left[\frac{\sin(\pi\alpha/2) - \cos(\pi\alpha/2)}{\cos(\pi\beta/2) - \sin(\pi\beta/2)} \right] \right)^{1/(\alpha-\beta)} \tag{10}$$

In Eq. (10), real solutions to ω_c exist only if $0 \leq \beta < 0.5 < \alpha \leq 1$ (Jaishankar and McKinley (2013)). If these constraints are not satisfied, it means that there is no crossover between the storage and loss moduli.

Once the linear viscoelasticity of the solutions have been characterized in this manner, we may now make predictions of the rheological response of the Xanthan gum solutions in other linear experiments. For example in creep tests, we apply a step stress of the form

$$\sigma(t) = \sigma_0 H(t) \tag{11}$$

where $H(t)$ is the Heaviside step function (Abramowitz and Stegun (1964)), and σ_0 is the magnitude of the step in the stress. For the case of the FMM, an analytical expression for the creep compliance $J(t)$ can be derived by substituting Eq. (11) in Eq. (5) and solving for $J(t) = \gamma(t)/\sigma_0$ (Schiessel *et al.* (1995); Jaishankar and McKinley (2013)). This is given by

$$J(t) \equiv \frac{\gamma(t)}{\sigma_0} = \frac{t^{\alpha}}{\mathbb{V}\Gamma(\alpha+1)} + \frac{t^{\beta}}{\mathbb{G}\Gamma(\beta+1)} \tag{12}$$

In Fig. 4 we show the measured creep compliance data (symbols) for 0.25 wt.% and 1 wt.% Xanthan gum solutions. The lines are *a priori* predictions obtained from the FMM by substituting the corresponding model values (taken from Tab. I) into Eq. (12). At short times the compliance increases as $J(t) \sim t^{\beta}$ whereas at long times the rate of creep increases, and $J(t) \sim t^{\alpha}$. The crossover between these regimes is gradual and depends on the values of $\mathbb{V}$, $\mathbb{G}$, α and β. Our prediction closely agrees with the measured data, and both of these power-law regimes are visible. At very short times $t \lessapprox 1$ s, the measured creep compliance

grows quadratically and overdamped periodic oscillations are observed. These oscillations, frequently referred to as creep ringing, arises from the coupling of instrument inertia with sample viscoelasticity (Ewoldt and McKinley (2007)). The initial quadratic response in the compliance arises purely due to the inertia of the measurement system and is given by $J(t) = (b/2I)t^2$, in which b is a geometry dependent measurement system factor and I is the total inertia of the spindle and the attached fixture. Because the initial quadratic response is material independent and is only a function of the attached fixture and system inertia, the short time response of both fluids coincide. However, the crossover from the short time inertia dominated response to the power-law response of the fluid occurs when

$$\frac{1}{2}\frac{b}{I}(t^*)^2 \approx \frac{(t^*)^\beta}{\mathbb{G}\Gamma(1+\beta)} \Rightarrow t^* \approx \left(\frac{2I/b}{\mathbb{G}\Gamma(1+\beta)}\right)^{1/(2-\beta)} \tag{13}$$

We have studied the creep ringing that is observed in power-law materials in detail in a previous publication, and have extended the inertia-less result above (Eq. (12)) to a prediction of the creep compliance for the Fractional Maxwell Model in the ringing regime (Jaishankar and McKinley (2013)). We note that for the times $t \gg 10^4$, the strain accumulated in the

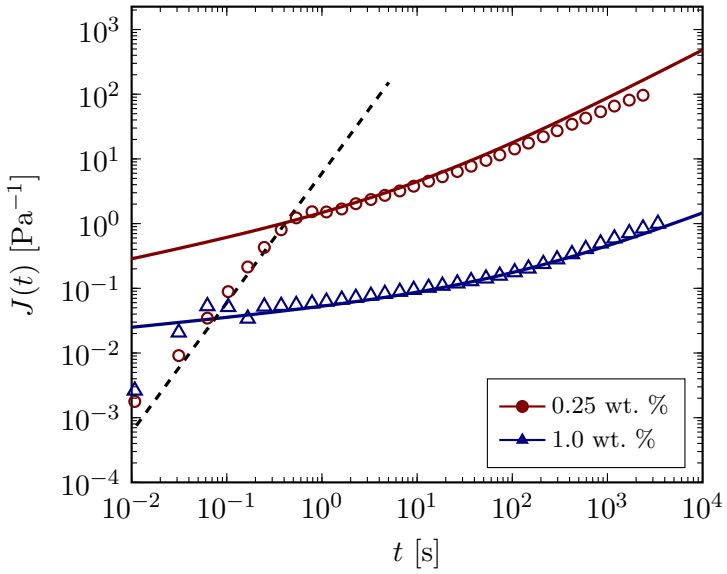

FIG. 4. Creep experiments performed on different concentrations of Xanthan gum (symbols) at an applied stress of $\sigma_0 = 0.01$ Pa, and the corresponding predictions of the linear viscoelastic creep compliance $J(t)$ (Eq. (12)). The values of the constitutive parameters $\alpha, \beta, \mathbb{V}$ and $\mathbb{G}$ used to make the prediction are obtained directly from the SAOS experiments (Tab. I). The initial quadratic response at short times is given by $J(t) = (b/2I)t^2$ and occurs due to the coupling of the instrument inertia with viscoelasticity, and is shown as a black dashed line.

Xanthan gum solution will become large enough at some point so that nonlinear effects may become important.

In a similar fashion, predictions of the relaxation modulus $G(t)$ and other linear viscoelastic material functions such as the transient viscosity $\eta^+(t)$ observed during start up of steady shear flow (Bird, Armstrong, and Hassager (1987)) can be made; we only require the parameter set (α, β, $\mathbb{V}$ and $\mathbb{G}$) that characterize the material. However, in each case, the material response will be independent of the magnitude of the imposed stress or strain amplitude. By contrast, experimental measurements on complex viscoelastic materials such as Xanthan gum solutions show a transition to strongly shear rate dependent material properties (Ross-Murphy (1995)) and we now seek to characterize this transition by generalizing the FMM to enable it to describe the rheological response to nonlinear deformations.

B. Nonlinear Viscoelasticity and the K-BKZ Model

When large nonlinear deformations are applied to complex fluids such as Xanthan gum, there is progressive loss of internal structure or damage to the equilibrium network in the material due to accumulated strain (Rolón-Garrido and Wagner (2009)). The material functions measured upon the application of a nonlinear strain are bounded by a linear viscoelastic envelope, and nonlinear material functions lie below this envelope. This damage or loss of internal structure is quantified by a monotonically decreasing *damping function* $h(\gamma)$, which we define below. We note that there are some polysaccharide systems that show thickening and hardening effects upon large strain deformations (Yalpani *et al.* (1983); Goh *et al.* (2007)). Such systems are beyond the scope of this work, but can be described by more complex functional forms of $h(\gamma)$. In the present study we focus on responses that are bounded by a linear viscoelastic envelope.

For the case of a steady shearing deformation, we may first evaluate this envelope by substituting into the constitutive equation for the FMM (Eq. (5)) the functional form of the deformation imposed during steady shear:

$$\dot{\gamma}(t) = \dot{\gamma}_0 H(t), \tag{14}$$

where $\dot{\gamma}_0$ is the steady shear rate applied at time $t = 0$ and $H(t)$ is the Heaviside step function. We therefore arrive at

$$\sigma(t) + \frac{\mathbb{V}}{\mathbb{G}} \frac{d^{\alpha-\beta}\sigma(t)}{dt^{\alpha-\beta}} = \mathbb{V}\dot{\gamma}_0 \frac{d^{\alpha-1}H(t)}{dt^{\alpha-1}} \tag{15}$$

Taking the Laplace transform (Podlubny (1999)) of (15) we obtain

$$\tilde{\sigma}(s) = \frac{\mathbb{V}\dot{\gamma}_0 s^{\alpha-2}}{1 + (\mathbb{V}/\mathbb{G})s^{\alpha-\beta}} \tag{16}$$

In deriving the Laplace transformed stress $\tilde{\sigma}(s)$ above, we have assumed initial conditions of $\gamma(0) = 0$ and $\dot{\gamma}(0) = 0$. We invert the transformed stress using known identities (Podlubny (1999); Valério *et al.* (2013)) to obtain

$$\eta^+(t) = \frac{\sigma(t)}{\dot{\gamma}_0} = \mathbb{G}t^{1-\beta} E_{\alpha-\beta,2-\beta}\left(-\frac{\mathbb{G}}{\mathbb{V}}t^{\alpha-\beta}\right) \tag{17}$$

We note two things here: first, that the steady shear viscosity is independent of the shear rate, as expected for a linear model and second, that the shear viscosity grows as a function of time and never reaches steady state, unless $\alpha = 1$. The Mittag-Leffler function asymptotically decays as $t^{-(\alpha-\beta)}$ (see Eq. (27)) for large arguments and hence $\eta^+(t) \sim t^{1-\alpha}$. This means that for the case of a dashpot with $\alpha = 1$, $\eta^+(t) \to \mathbb{V}(= \eta)$ at long times.

To be able to capture experimental observation of the shear rate dependence of the viscosity, and to be able to obtain an equilibrium steady state viscosity, we need to incorporate into our model a frame invariant finite strain measure. We follow the approach of Larson (1985) who argued that the nonlinear rheology of complex multiscale materials such as polydisperse polymer melts can be described by using a separable equation of the integral K-BKZ type (Bird, Armstrong, and Hassager (1987)). While Larson selected a single power-law relaxation kernel, we extend the analysis to relaxation kernels of the Mittag-Leffler kind. By assuming that the temporal response and strain response are separable or factorizable, so that the stress tensor $\boldsymbol{\sigma}(t)$ can be written as (Bird, Armstrong, and Hassager (1987); Larson (1988))

$$\boldsymbol{\sigma}(t) = \int_{-\infty}^{t} m(t-t') \left[2\frac{\partial U}{\partial I_1}\boldsymbol{C}^{-1} - 2\frac{\partial U}{\partial I_2}\boldsymbol{C}\right] dt' \tag{18}$$

in which

$$m(t-t') = \frac{\partial G(t-t')}{\partial t'} \tag{19}$$

is the memory function of the material, $U \equiv U(I_1, I_2)$ is a potential function that is related to the strain energy function of the material and $\boldsymbol{C}^{-1} = (\boldsymbol{F}^{-1})^T \cdot \boldsymbol{F}$ is the Finger tensor (Bird, Armstrong, and Hassager (1987)). If we neglect the second term in brackets, i.e. the potential function have no dependence on the second invariant I_2, (Wagner, Raible, and Meissner (1979)), then for the specific kinematics of a shear deformation, the expression for the shear stress can be written as (Larson (1988))

$$\sigma(t) = \int_{-\infty}^{t} m(t-t')h(\gamma)\gamma(t,t')\ dt' \tag{20}$$

in which $\gamma(t,t') = \gamma(t') - \gamma(t)$ is the relative strain accumulated between times t and t' and $h(\gamma)$ is a damping function defined as

$$h(\gamma) = \frac{G(t,\gamma)}{G(t)}. \tag{21}$$

Many polymer kinetic theories can be rewritten in the form of the separable K-BKZ integral equations defined above, including the Rouse-Zimm theory and the Lodge network theory (Bird, Armstrong, and Hassager (1987)). The challenge lies in determining a molecular basis for the memory function $m(t-t')$. In what follows we select the Mittag-Leffler relaxation kernel as the appropriate memory function for our biopolymer solutions, i.e., we set

$$m(t-t') \equiv \frac{\partial G(t-t')}{\partial t} \tag{22}$$

$$= -\mathbb{G}(t-t')^{-1-\beta} E_{\alpha-\beta,-\beta}\left(-\frac{\mathbb{G}}{\mathbb{V}}(t-t')^{\alpha-\beta}\right). \tag{23}$$

where we have used $G(t)$ from Eq. (8). Although our choice of the memory function is motivated by experimental data, and the large number of publications that have shown that complex multiscale materials exhibit relaxation of the Mittag-Leffler kind, a micro-molecular basis for this kind of relaxation process in polymeric materials has been recently proposed by Sharma and Cherayil (2010).

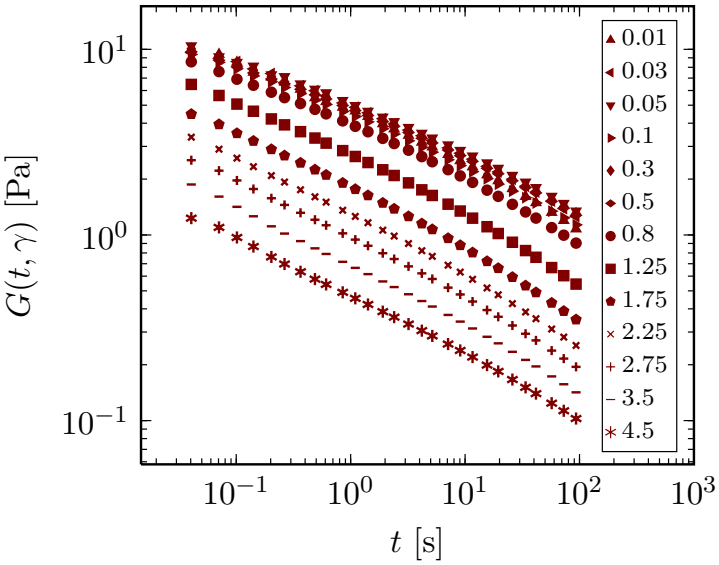

FIG. 5. Relaxation modulus $G(t)$ obtained from step strain experiments performed on a 0.5 wt.% Xanthan gum solution at different strain amplitudes. The legend box shows the strain amplitude γ_0 at which the stress relaxation test was performed. Increasing the strain amplitude causes a progressive decrease in the relaxation modulus, which can be quantified using a damping function of the form given by Eq. (21).

In order to calculate the steady shear viscosity from Eq. (20), we need to determine the damping function $h(\gamma)$ for our Xanthan gum solutions. For this we performed a series of stress relaxation experiments with increasing step strain, and the results for a 0.5 wt.% solution are shown in Fig. 5. Note that here too we can detect the signature of two distinct limiting power-law regimes during relaxation, with a gradual cross over from one to the other occurring at times of order $\tau \sim (\mathbb{V}/\mathbb{G})^{1/(\alpha-\beta)}$. At small strain amplitudes ($\gamma_0 < 0.3$), the step strain experiments yield a relaxation modulus that is independent of strain amplitude, indicating a linear viscoelastic response. However, upon increasing the strain amplitude, we observe a progressive decrease in the relaxation modulus $G(t,\gamma)$. We may collapse these curves generated at different strain amplitudes onto a single master curve, and in the process experimentally determine the damping function $h(\gamma)$, which is given by Eq. (21). We show the measured value of the damping function $h(\gamma)$ as a function of strain amplitude γ for 0.25, 0.5 and 1.0 wt.% Xanthan gum solutions in Fig. 6. The damping functions for all concentrations of Xanthan gum tested in this study overlap on each other and fall on the same master curve. The damping function is independent of strain for small values of applied step strain; however at strains of $\gamma \approx 30\%$, $h(\gamma)$ drops sharply and approaches a power-law

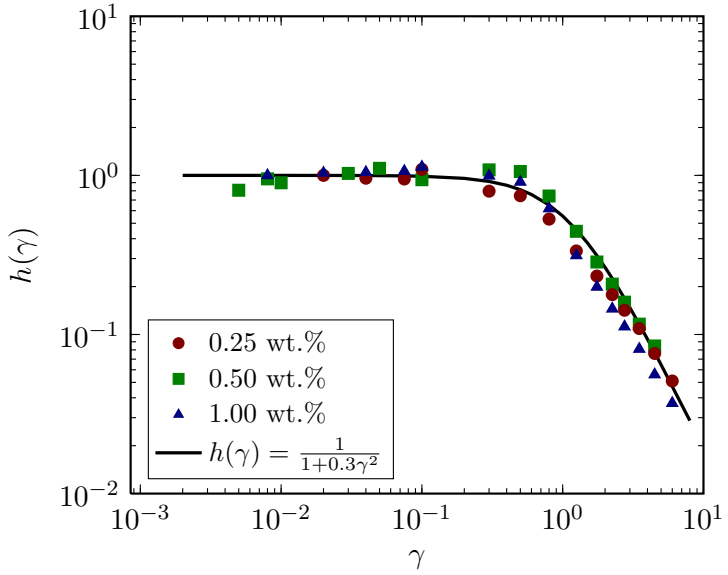

FIG. 6. Measured values of the damping function $h(\gamma) = G(t,\gamma)/G(t)$ for different concentrations of Xanthan Gum. The damping function is independent of concentration and is well described by a function of the form $h(\gamma) = 1/(1 + 0.3\gamma^2)$.

function of the applied strain for large γ. We have independently verified that non-linearity appears at $\gamma_0 = 30\%$ using a strain amplitude sweep under SAOS deformations. The black line in Fig. 6 indicates a fit to this master curve with a function of the form

$$h(\gamma) = \frac{1}{1 + a\gamma^2}. \tag{24}$$

and we find that $a = 0.3$ describes our data well. Rolón-Garrido and Wagner (2009) have recently reviewed the various kinds of damping functions that arise in rheology and their role in describing non-linear rheological behavior. A damping function of the form $h(\gamma) = 1/(1 + a\gamma^b)$ where a and b are constants has been commonly observed in a number of other polymeric systems (Soskey and Winter (1984)).

We now have all the elements required to find the steady shear viscosity $\eta(\dot{\gamma})$ using Eq. (20). We substitute Eq. (23) and Eq. (24) into Eq. (20) and also note that $\gamma(t,t') =$

$\gamma(t') - \gamma(t) = \dot{\gamma}(t - t')$ for steady shearing flow to arrive at

$$\eta(\dot{\gamma}) \equiv \frac{\sigma(t)}{\dot{\gamma}}$$
$$= -\mathbb{G} \int_0^\infty u^{-\beta} E_{\alpha-\beta,-\beta}\left(-\frac{\mathbb{G}}{\mathbb{V}} u^{\alpha-\beta}\right) \frac{1}{1 + 0.3(\dot{\gamma}u)^2}\, du \tag{25}$$

in which we have made the variable transformation $u = t - t'$. The above integral for $\eta(\dot{\gamma})$ is evaluated numerically and can be shown to converge for all values of $\dot{\gamma}$. We note that to evaluate this integral for each fluid no additional fitting parameters are required, and we use the corresponding values of $\alpha, \beta, \mathbb{V}$ and $\mathbb{G}$ from Tab. I, which were obtained using SAOS experiments.

In Fig. 7a we show measured data (symbols) for the steady shear viscosity $\eta(\dot{\gamma})$ as a function of the steady shear rate $\dot{\gamma}$ for different concentrations of Xanthan gum in solution. For all concentrations tested, $\eta(\dot{\gamma})$ displays either one (1 wt. %) or two (0.25 wt.% and 0.5 wt.%) distinct power-law regions. Moreover there is no appearance of a zero shear viscosity plateau even at shear rates as low as $\dot{\gamma} = 10^{-3}$ s^{-1}, with $\eta(\dot{\gamma})$ continuing to grow as a weak power-law function of $\dot{\gamma}$ as the shear rate is progressively decreased. This asymptotic power-law behavior with the absence of a well-defined zero-shear plateau has been documented previously for Xanthan gum solutions (Ross-Murphy (1995); Oertel and Kulicke (1991)) as well as for other complex fluids such as liquid crystalline polymers (Guskey and Winter (1991)) and associative polymer solutions (English *et al.* (1999)). We also show in Fig. 7a the predictions of $\eta(\dot{\gamma})$ obtained from the K-BKZ model described above (Eq. (25)). The predicted material response captures the behavior of the Xanthan gum solutions very closely.

We may gain additional analytical insight into the asymptotic behavior of the flow curve by approximating the integral in Eq. (25). We begin by noting that the Mittag-Leffler function has the following asymptotic behavior (Podlubny, 1999, pp. 17 and pp. 34):

$$E_{a,b}(z) \approx \sum_{k=0}^{N} \frac{z^k}{\Gamma(ak + b)} + O(z^{N+1});\ z \ll 1 \tag{26}$$

$$E_{a,b}(z) \approx \sum_{k=1}^{N} \frac{(-z)^{-k}}{\Gamma(b - ak)} + O(z^{-(N+1)});\ z \gg 1 \tag{27}$$

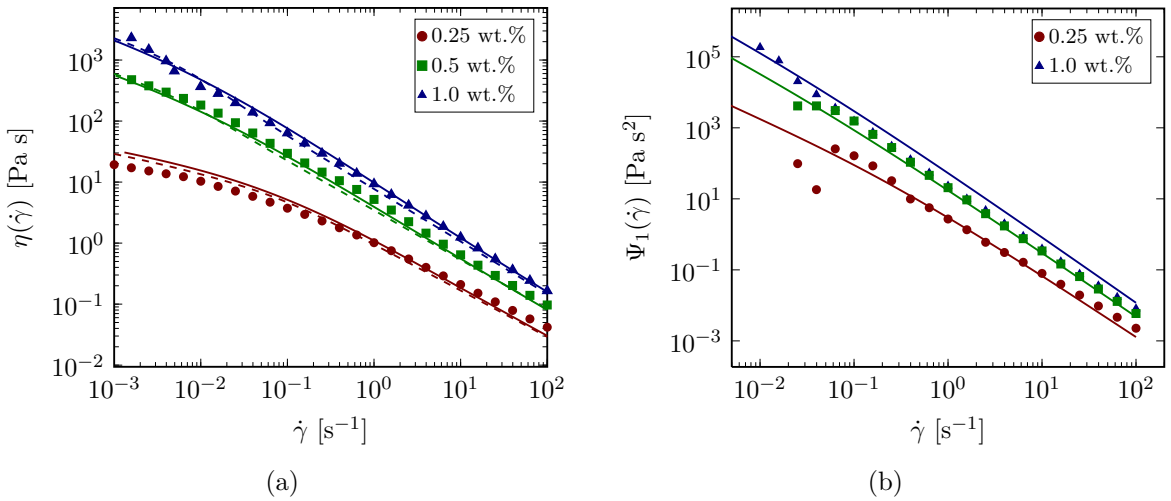

FIG. 7. Predictions of nonlinear material functions using the K-BKZ type model (lines) compared with measured data (symbols); (a) steady shear viscosity $\eta(\dot{\gamma})$, and (b) first normal stress coefficient $\Psi_1(\dot{\gamma})$. The model parameters for each fluid are determined from linear viscoelasticity and are given in Tab. I. The dashed lines in (a) show the viscosity given by the asymptotic simplification in Eq. (32).

We make use of these asymptotes to evaluate Eq. (25) by approximating the Mittag-Leffler function in Eq. (25) as being a piecewise continuous function of the form

$$\begin{aligned} E_{\alpha-\beta,-\beta}\left(-\frac{\mathbb{G}}{\mathbb{V}}u^{\alpha-\beta}\right) &= \frac{1}{\Gamma(-\beta)} \qquad ; u < u^* \\ &= \frac{(\mathbb{V}/\mathbb{G})u^{\beta-\alpha}}{\Gamma(-\alpha)}; \ u \geq u^* \end{aligned} \tag{28}$$

where u^* is the location of the cross over from one asymptote to the other. We assume this crossover occurs when the argument of the Mittag-Leffler function $z^* = (\mathbb{V}/\mathbb{G})^{1/(\alpha-\beta)}u^* \sim 1$, i.e., $u^* = (\mathbb{V}/\mathbb{G})^{1/(\alpha-\beta)} = \tau$. Therefore we now approximate Eq. (25) as

$$\eta(\dot{\gamma}) \approx -\mathbb{G}\dot{\gamma}^{\beta-1}\left[\int_0^{\gamma^*}\gamma^{-\beta}\frac{1}{\Gamma(-\beta)}\frac{1}{1+0.3\gamma^2}\,d\gamma + \int_{\gamma^*}^{\infty}\gamma^{-\beta}\frac{\left((\mathbb{V}/\mathbb{G})\dot{\gamma}^{\alpha-\beta}\gamma^{\beta-\alpha}\right)}{\Gamma(-\alpha)}\,d\gamma\right]. \tag{29}$$

In deriving the above, we have made the variable substitution $\dot{\gamma}u = \gamma$ for steady shear flow, and consequently $\gamma^* = (\mathbb{V}/\mathbb{G})^{1/(\alpha-\beta)}\dot{\gamma} = \tau\dot{\gamma}$. Note that γ^* is a product of a timescale τ and a shear rate $\dot{\gamma}$ and hence $\gamma^* = \tau\dot{\gamma}$ may be interpreted as a critical shear strain during start up of steady shear at a rate $\dot{\gamma}$, or as a Weissenberg number Wi that gives a measure of the

flow strength (Dealy (2010)). Upon simplifying Eq. (29) we arrive at

$$\eta(\dot{\gamma}) \approx \mathbb{G}\dot{\gamma}^{\beta-1}\frac{\beta}{\Gamma(1-\beta)}\int_0^{\gamma^*}\frac{\gamma^{-\beta}}{1+0.3\gamma^2}\,d\gamma + \mathbb{V}\dot{\gamma}^{\alpha-1}\frac{\alpha}{\Gamma(1-\alpha)}\int_{\gamma^*}^{\infty}\frac{\gamma^{-\alpha}}{1+0.3\gamma^2}\,d\gamma \tag{30}$$

where we have used the identity $\Gamma(n+1) = n\Gamma(n)$. Both the integrals obtained above can be written in terms of the hypergeometric function ${}_2F_1(a,b;c;x)$ defined as (Abramowitz and Stegun (1964))

$${}_2F_1(a,b;c;z) = \frac{\Gamma(c)}{\Gamma(a)\Gamma(b)}\sum_{k=0}^{\infty}\frac{\Gamma(a+k)\Gamma(b+k)}{\Gamma(c+k)}\frac{z^k}{k!} \tag{31}$$

and we finally obtain

$$\begin{aligned}\eta(\dot{\gamma}) \approx \mathbb{G}\dot{\gamma}^{\beta-1}\frac{\beta}{\Gamma(1-\beta)}\frac{(\gamma^*)^{1-\beta}}{1-\beta}\,{}_2F_1\left(1,\frac{1-\beta}{2};\frac{3-\beta}{2};-0.3(\gamma^*)^2\right) + \\ \mathbb{V}\dot{\gamma}^{\alpha-1}\frac{\alpha}{\Gamma(1-\alpha)}\frac{(\gamma^*)^{-\alpha-1}}{(0.3)(1+\alpha)}\,{}_2F_1\left(1,\frac{1+\alpha}{2};\frac{3+\alpha}{2};-\frac{1}{0.3(\gamma^*)^2}\right).\end{aligned} \tag{32}$$

We show the predictions of this approximate analytic expression for $\eta(\dot{\gamma})$ as dotted lines in Fig. 7a. It is observed that this analytical solution agrees very closely with the full numerical solution and hence one may avoid calculating a numerical solution to Eq. (25). For values of $\alpha \approx 1$ or $\beta \approx 0$, this approximate solution is less accurate; in the Appendix we derive an expression for $\eta(\dot{\gamma})$ to arbitrary order, and one may retain as many terms as required in the expansion depending on the accuracy needed. The utility of the analytical solution Eq. (32) is that it enables us to calculate the asymptotic behavior of $\eta(\dot{\gamma})$ as $\mathrm{Wi} \ll 1$ and $\mathrm{Wi} \gg 1$; in fact, it can be shown using appropriate Taylor series expansions of the hypergeometric functions that at low shear rate

$$\lim_{\dot{\gamma}\ll 1/\tau}\eta(\dot{\gamma}) \approx \left[(0.3)^{(\alpha-1)/2}\frac{(\pi\alpha/2)\sec(\pi\alpha/2)}{\Gamma(1-\alpha)}\right]\mathbb{V}\dot{\gamma}^{\alpha-1} \tag{33}$$

and at high shear rate

$$\lim_{\dot{\gamma}\gg 1/\tau}\eta(\dot{\gamma}) \approx \left[(0.3)^{(\beta-1)/2}\frac{(\pi\beta/2)\sec(\pi\beta/2)}{\Gamma(1-\beta)}\right]\mathbb{G}\dot{\gamma}^{\beta-1} \tag{34}$$

From Eq. (33), it is apparent that the existence of a constant bounded viscosity in the limit

of zero shear rate thus only exists for materials in which $\alpha = 1$. The shear stress however tends to zero for all α because $\sigma = \eta\dot{\gamma} \sim \dot{\gamma}^{\alpha}$ for all α. This slow asymptotic divergence in the viscosity at low shear rates agrees with the experimentally observed behavior of many complex multiscale materials, some of which have been cited above.

The K-BKZ approach also enables us to make predictions of the first normal stress coefficient $\Psi_1(\dot{\gamma})$. Again, we begin with the K-BKZ framework (Eq. (18)), and neglect the second term for uncrosslinked materials. We select the correct components of the Finger tensor $\boldsymbol{C}^{-1}$ to calculate the normal stress difference $N_1 = \sigma_{xx} - \sigma_{yy}$ and we obtain (Venkataraman and Winter (1990))

$$N_1(t) = \int_{-\infty}^{t} m(t-t')h(\gamma)\gamma^2(t,t')\ dt' \tag{35}$$

and consequently, substituting the Mittag-Leffler relaxation modulus we obtain

$$\Psi_1(\dot{\gamma}) \equiv \frac{N_1}{\dot{\gamma}^2} = -\mathbb{G}\int_0^{\infty} u^{1-\beta}E_{\alpha-\beta,-\beta}\left(-\frac{\mathbb{G}}{\mathbb{V}}u^{\alpha-\beta}\right)\frac{1}{1+0.3(\dot{\gamma}u)^2}\ du \tag{36}$$

In Fig. 7b we show measurements of the first normal stress coefficient $\Psi_1(\dot{\gamma})$ (symbols) for three different concentrations of Xanthan gum in solution. The solid lines show the numerical prediction of $\Psi_1(\dot{\gamma})$ evaluated using Eq. (36) and the parameters in Tab. I. In this case too we observe that the agreement between measured data and the prediction of our model is good with no additional fitting parameters required. Similar to the approximation made above for $\eta(\dot{\gamma})$, an analytical approximation for $\Psi_1(\dot{\gamma})$ may be found, and is given by

$$\begin{aligned}\Psi_1(\dot{\gamma}) \approx \mathbb{G}\dot{\gamma}^{\beta-2}\frac{\beta}{\Gamma(1-\beta)}\frac{(\gamma^*)^{2-\beta}}{2-\beta}{}_2F_1\left(1,\frac{2-\beta}{2};\frac{4-\beta}{2};-0.3(\gamma^*)^2\right)+\\ \mathbb{V}\dot{\gamma}^{\alpha-2}\frac{\alpha}{\Gamma(1-\alpha)}\frac{(\gamma^*)^{-\alpha}}{(0.3)(\alpha)}{}_2F_1\left(1,\frac{\alpha}{2};\frac{2+\alpha}{2};-\frac{1}{0.3(\gamma^*)^2}\right)\end{aligned} \tag{37}$$

As before, $\gamma^* = (\mathbb{V}/\mathbb{G})^{1/(\alpha-\beta)}\dot{\gamma} = \tau\dot{\gamma}$ is a measure of the flow strength. This approximate analytical solution is nearly identical to the full numerical solution of Eq. (36), and the numerical and analytical curves overlap; therefore, we do not show the approximate solution as dashed lines for the sake of clarity. Again, with the help of the analytical solution we are

able to determine the behavior of $\Psi_1(\dot{\gamma})$ for $\mathrm{Wi} \ll 1$ given by

$$\lim_{\dot{\gamma} \ll 1/\tau} \Psi_1(\dot{\gamma}) \approx \left[(0.3)^{(\alpha-2)/2} \frac{(\pi\alpha/2)\mathrm{cosec}(\pi\alpha/2)}{\Gamma(1-\alpha)} \right] \mathbb{V} \dot{\gamma}^{\alpha-2} \tag{38}$$

and for $\gamma^* \gg 1$

$$\lim_{\dot{\gamma} \gg 1/\tau} \Psi_1(\dot{\gamma}) \approx \left[(0.3)^{(\beta-2)/2} \frac{(\pi\beta/2)\mathrm{cosec}(\pi\beta/2)}{\Gamma(1-\beta)} \right] \mathbb{V} \dot{\gamma}^{\beta-2} \tag{39}$$

i.e. $\Psi_1(\dot{\gamma}) \sim \dot{\gamma}^{\alpha-2}$ for $\gamma^* \ll 1$ and $\Psi_1(\dot{\gamma}) \sim \dot{\gamma}^{\beta-2}$ for $\gamma^* \gg 1$. We note in particular that the asymptotic behavior of $\Psi_1(\dot{\gamma})$ at low shear rates obtained above agrees with the asymptote calculated from a second order fluid expansion (Bird, Armstrong, and Hassager (1987))

$$\lim_{\dot{\gamma} \ll 1/\tau} \Psi_1(\dot{\gamma}) = \lim_{\omega \ll 1/\tau} \frac{2G'(\omega)}{\omega^2} \tag{40}$$

which we can calculate with the help of Eq. (6).

In this section we have presented a theoretical constitutive framework to make predictions of the nonlinear rheological response of power-law complex fluids with broad relaxation spectra that exhibit liquid-like behavior at long timescales. Although we discuss the examples of $\eta(\dot{\gamma})$ and $\Psi_1(\dot{\gamma})$ in this paper, these arguments can be extended to other nonlinear deformations such as uniaxial extensional flows and LAOS. We next discuss the performance of empirical rules such as the Cox-Merz rule and the Gleissle Mirror relations that also make predictions of a material's nonlinear response (from knowledge of the linear rheology alone), and show how the very broad range of relaxation timescales that are embodied by the Mittag-Leffler function influences the validity of these approximations. We will also put these empirical rules in context by using our model to quantify the systematic deviations that these predictions can exhibit from measured data.

C. Empirical Relationships for Nonlinear Viscoelasticity

One widely known relationship that enables the prediction of the nonlinear viscometric response for complex materials from linear response is the Cox-Merz rule which states that

(Bird, Armstrong, and Hassager (1987))

$$\eta(\dot{\gamma}) \approx \eta^*(\omega)\big|_{\omega=\dot{\gamma}} \tag{41}$$

where $\eta^*(\omega)$ is the complex viscosity given by

$$\eta^*(\omega) = \frac{\sqrt{G'(\omega)^2 + G''(\omega)^2}}{\omega} \tag{42}$$

For the FMM, in which $G'(\omega)$ and $G''(\omega)$ are given by Eq. (6) and Eq. (7) respectively, we calculate $\eta^*(\omega)$ to be

$$\eta^*(\omega) = \frac{\mathbb{V}\mathbb{G}\omega^{\alpha+\beta-1}}{\sqrt{(\mathbb{V}\omega^{\alpha})^2 + (\mathbb{G}\omega^{\beta})^2 + 2\mathbb{V}\omega^{\alpha}\mathbb{G}\omega^{\beta}\cos\left(\frac{\pi(\alpha-\beta)}{2}\right)}} \tag{43}$$

and consequently from (41) we have

$$\eta(\dot{\gamma}) \approx \frac{\mathbb{V}\mathbb{G}\dot{\gamma}^{\alpha+\beta-1}}{\sqrt{(\mathbb{V}\dot{\gamma}^{\alpha})^2 + (\mathbb{G}\dot{\gamma}^{\beta})^2 + 2\mathbb{V}\dot{\gamma}^{\alpha}\mathbb{G}\dot{\gamma}^{\beta}\cos\left(\frac{\pi(\alpha-\beta)}{2}\right)}} \tag{44}$$

There also exists a less widely used empirical framework to predict nonlinear behavior from linear rheology, collectively known as the Gleissle mirror relations which state that (Bird, Armstrong, and Hassager (1987); Dealy and Wissbrun (1990))

$$\eta^+(t) \approx \eta(\dot{\gamma})\Big|_{t=1/\dot{\gamma}} \tag{45}$$

$$\Psi_1^+(t) \approx \Psi_1(\dot{\gamma})\Big|_{t=k/\dot{\gamma}} \tag{46}$$

$$\Psi_1(\dot{\gamma}) \approx -2\int_{\dot{\gamma}/k}^{\infty} x^{-1}\left[\frac{\partial\eta(x)}{\partial x}\right]\, dx \tag{47}$$

Here $\eta^+(t)$ is the transient shear viscosity upon the start-up of steady shear measured in the linear viscoelastic regime and $\Psi_1^+(t)$ is the transient first normal stress coefficient upon the start-up of steady shear, and $2 < k < 3$ is a fitting constant. Evidently, these Gleissle mirror relations allow estimation of the nonlinear material functions $\eta(\dot{\gamma})$ and $\Psi_1(\dot{\gamma})$ from their quasilinear counterparts $\eta^+(t)$ and $\Psi_1^+(t)$. The third relation Eq. (47) allows a direct

calculation of $\Psi_1(\dot{\gamma})$ from $\eta(\dot{\gamma})$. For the FMM, we have already determined $\eta^+(t)$ in Eq. (17), because in deriving that expression we set $\dot{\gamma} = \dot{\gamma}_0 H(t)$, which is the imposed deformation in a start-up of steady shear flow experiment. Therefore Eq. (17) and Eq. (45) yield

$$\eta(\dot{\gamma}) \cong \mathbb{G}\left(\frac{1}{\dot{\gamma}}\right)^{1-\beta} E_{\alpha-\beta,2-\beta}\left(-\frac{\mathbb{G}}{\mathbb{V}}\left(\frac{1}{\dot{\gamma}}\right)^{\alpha-\beta}\right) \tag{48}$$

in which $E_{a,b}(z)$ is the Mittag-Leffler function defined in Eq. (9). The argument $z = -\frac{\mathbb{G}}{\mathbb{V}}\left(\frac{1}{\dot{\gamma}}\right)^{\alpha-\beta}$ in Eq. (48) can also be written as $z = -(\tau\dot{\gamma})^{\beta-\alpha}$. It can be shown using the asymptotic forms of the Mittag-Leffler function given in Eq. (26) and Eq. (27) that Eq. (48) exhibits power-law regimes at low as well as high $\dot{\gamma}$. At low shear rates we obtain

$$\lim_{\dot{\gamma}\ll 1/\tau} \eta(\dot{\gamma}) \approx \mathbb{V}\dot{\gamma}^{\alpha-1}/\Gamma(2-\alpha), \tag{49}$$

and at high rates we find

$$\lim_{\dot{\gamma}\gg 1/\tau} \eta(\dot{\gamma}) \approx \mathbb{G}\dot{\gamma}^{\beta-1}/\Gamma(2-\beta). \tag{50}$$

These asymptotes are identical in form to those we obtained from the K-BKZ model derived above (cf. Eqs. (33) and (34)) and only differ in the pre-multiplying factor.

We may now use this expression for $\eta(\dot{\gamma})$ in Eq. (47) to find $\Psi_1(\dot{\gamma})$. Making this substitution we have

$$\Psi_1(\dot{\gamma}) = -2\int_{\dot{\gamma}/k}^{\infty} \frac{1}{x}\frac{\partial}{\partial x}\left[\mathbb{G}\left(\frac{1}{x}\right)^{1-\beta} E_{\alpha-\beta,2-\beta}\left(-\frac{\mathbb{G}}{\mathbb{V}}\left(\frac{1}{x}\right)^{\alpha-\beta}\right)\right] dx \tag{51}$$

Making the variable transformation $1/x = u$ and then integrating by parts we obtain

$$\Psi_1(\dot{\gamma}) = 2\mathbb{G}\left(\frac{k}{\dot{\gamma}}\right)^{2-\beta}\left[E_{\alpha-\beta,2-\beta}\left(-\frac{\mathbb{G}}{\mathbb{V}}\left(\frac{k}{\dot{\gamma}}\right)^{\alpha-\beta}\right) - E_{\alpha-\beta,3-\beta}\left(-\frac{\mathbb{G}}{\mathbb{V}}\left(\frac{k}{\dot{\gamma}}\right)^{\alpha-\beta}\right)\right] \tag{52}$$

As in the case of $\eta(\dot{\gamma})$, it can be shown that the low and high shear rate asymptotes are both power-laws, and are given by $\Psi_1(\dot{\gamma}) \sim \dot{\gamma}^{\alpha-2}$ and $\Psi_1(\dot{\gamma}) \sim \dot{\gamma}^{\beta-2}$ respectively. These asymptotic power-laws agree with those of the K-BKZ model derived in Eq. (38) and Eq. (39).

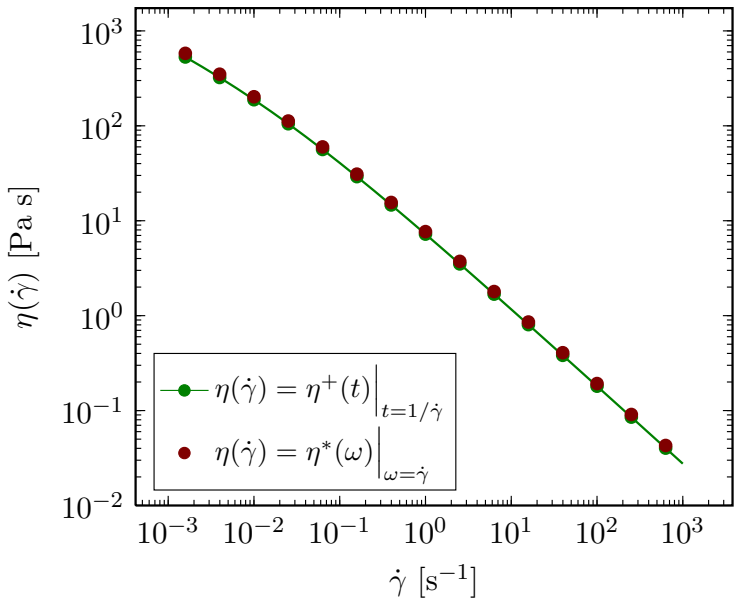

FIG. 8. Comparison of the agreement between the Cox-Merz rule and the Gleissle mirror relations for the FMM. The predicted values of the steady shear viscosity from the two different rules virtually overlap. Additional arguments for this agreement are given in appendix. $\alpha = 0.64$, $\beta = 0.19$, $\mathbb{V} = 71.65$ Pa s$^\alpha$, $\mathbb{G} = 7.82$ Pa s$^\beta$.

In Fig. 8 we show a comparison of the prediction of $\eta(\dot\gamma)$ from the Cox-Merz rule (Eq. (44)) with the prediction of the Gleissle mirror relation (Eq. (48)) for the special case of $\alpha = 0.64$, $\beta = 0.19$, $\mathbb{V} = 71.65$ Pa s$^\alpha$ and $\mathbb{G} = 7.82$ Pa s$^\beta$, corresponding to a 0.5 wt.% Xanthan gum solution. The two predictions agree very closely over 6 orders of magnitude in the deformation rate. We have verified for various other values of α, β, $\mathbb{V}$ and $\mathbb{G}$ that the two predictions are nearly equal at all shear rates. Therefore we may use either the Cox-Merz rule or the Gleissle mirror relations to arrive at an empirical prediction of the nonlinear material properties $\eta(\dot\gamma)$ and $\Psi_1(\dot\gamma)$ for a multiscale material with linear viscoelastic properties described by the Fractional Maxwell Model.

In Fig. 9 we show as symbols the same steady shear data measured for two different concentrations of Xanthan gum already presented in Fig. 7. The lines in Fig. 9 depict the predictions obtained from the Gleissle mirror relations (Eqs. (48) and (52)). Note that although we do not show it in Fig. 9 for the sake of clarity, applying the Cox-Merz rule (Eq. (41)) would give us identical predictions as the Gleissle mirror relation as explained above. We choose to show the predictions of the Gleissle mirror relations because this also provides an analytical expression for $\Psi_1(\dot\gamma)$, however all of the conclusions in the following section apply to the Cox-Merz rule as well.

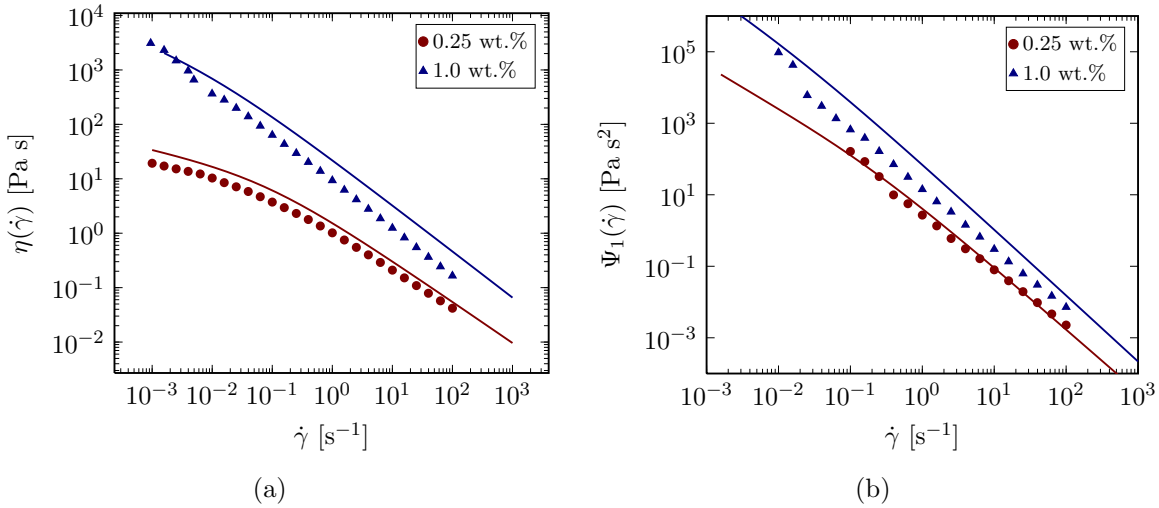

FIG. 9. Predictions of the Gleissle mirror relations for the FMM (lines) compared to measured data for Xanthan gum(symbols); (a) steady shear viscosity $\eta(\dot{\gamma})$ prediction (Eq. (48)) and (b) first normal stress co-efficient $\Psi_1(\dot{\gamma})$ prediction (Eq. (52)). There is a consistent offset between the prediction and measured data, which increases with increasing concentration. Values of α, β, $\mathbb{V}$ and $\mathbb{G}$ used to make the model predictions were taken from Tab. I.

We observe in Fig. 9 that the predictions of the Gleissle mirror relations correctly capture the functional form of the experimental data but exhibit a systematic offset from the measurements in both $\eta(\dot{\gamma})$ (Fig. 9a) as well as $\Psi_1(\dot{\gamma})$ (Fig. 9b). The predictions are systematically higher than the measured data. This offset between measured data and the predictions of empirical rules such as the Cox-Merz rule or Gleissle mirror relations has been observed previously in various complex fluids, especially in polysaccharide systems where it has been reported that $\eta^*(\omega)|_{\omega=\dot{\gamma}} > \eta(\dot{\gamma})$. For Xanthan gum solutions this offset has been shown to increase with increasing Xanthan concentration (Ross-Murphy (1995)). Using Xanthan gum and Schizophyllum solutions with varying amounts of urea (Ross-Murphy, Morris, and Morris (1983)) or DMSO (Oertel and Kulicke (1991)) respectively, this offset has been shown to arise from the presence of intermolecular interactions such as hydrogen bonds. These weak physical interactions give rise to the broad power-law–like characteristics we observe in the linear relaxation modulus, but are disrupted at the large strain deformations applied in steady shear.

In our K-BKZ model, we capture this structural damage accumulated during large shear deformations using the damping function. With this K-BKZ framework, it is also relatively straightforward to quantify the magnitude of this offset between the measured steady shear viscosity and the predictions of the Cox-Merz rule or Gleissle mirror relations. We define

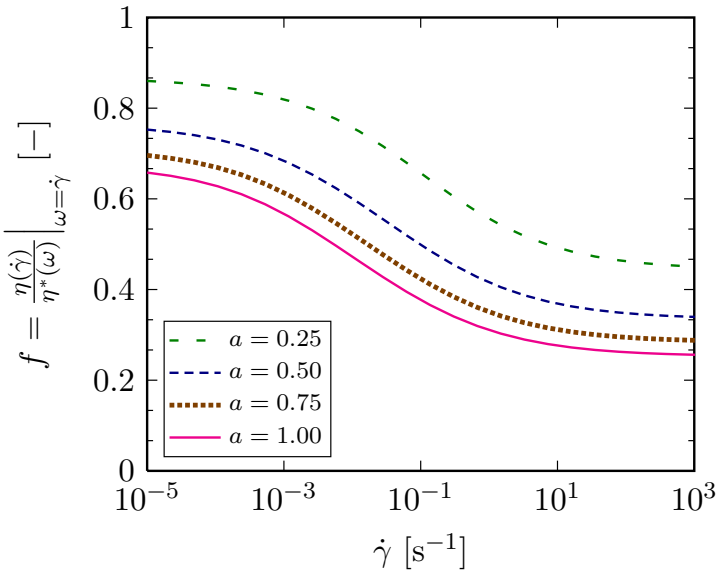

FIG. 10. The offset factor f (Eq. (53)) as a function of the shear rate $\dot\gamma$ for different values of the damping function parameter a. $0 < f < 1$ indicating that the steady shear viscosity is lower than the complex viscosity. This arises from damage accumulated at the large strains imposed during a steady shear experiment. The values of the FMM parameters are $\alpha = 0.60$, $\beta = 0.14$, $\mathbb{V} = 208.54$ Pa s$^\alpha$ and $\mathbb{G} = 22.46$ Pa s$^\beta$ corresponding to the 1 wt.% Xanthan gum solution with characteristic timescale $\tau = (\mathbb{V}/\mathbb{G})^{1/(\alpha-\beta)} = 1846$ s.

the offset factor f as

$$f \equiv \frac{\eta(\dot\gamma)}{\eta^*(\omega)}\Big|_{\omega=\dot\gamma} \tag{53}$$

where $\eta(\dot\gamma)$ and $\eta^*(\omega)\big|_{\omega=\dot\gamma}$ are given by Eqs. (25) and (44)) respectively. We could also replace $\eta^*(\omega)\big|_{\omega=\dot\gamma}$ by $\eta(\dot\gamma)$ obtained from the Gleissle mirror relationship (Eq. (48)) because both empirical relations give nearly identical predictions of the steady shear viscosity (cf. Fig. 8). Note that as long as $0 < f < 1$, the smaller the value of f, the larger is the deviation between $\eta(\dot\gamma)$ and $\eta^*(\omega)$. We show the value of f as a function of shear rate $\dot\gamma$ for various values of the strain damping coefficient a in Fig. 10. We do not compare this plot of the offset with our measured data because that would mean plotting the ratio of two measured quantities on the y-axis. Moreover, the y-axis only ranges from 0 to 1; it can be calculated that even a 5-6% error in both $\eta(\dot\gamma)$ and $\eta^*(\omega)$, which is a reasonable assumption to make in bulk rheology, can lead to as much as a 25% error in the calculated offset. Nevertheless, from Fig. 10 we can discern various qualitative features: the introduction of the damping function leads to a systematic offset of magnitude $0.3 \leq f \leq 0.9$ between the Cox-Merz

prediction and the full nonlinear model. Similar offsets were found experimentally for all the Xanthan gum concentrations tested in this study. The offset factor f also monotonically decreases as a function of $\dot{\gamma}$. We see from Fig. 9(a) that this is true for the 1 wt.%, and 0.5 wt.% (not shown for clarity); however, the trend seems to be reversed for the 0.25 wt.% solution, which we ascribe to experimental variability. The magnitude of this offset also plateaus at both low and high $\dot{\gamma}$. These plateaus indicate that approximations to the steady shear viscosity obtained from these empirical relationships will exhibit asymptotic behavior (to within a constant factor) that is identical to the full K-BKZ model, which compares well with experimental measurements. In fact, using our analytical solution, we can show this exactly; the plateau values of the offset may be calculated from the asymptotic values of $\eta(\dot{\gamma})$ from the K-BKZ model (Eqs. (33) and (34)) and those of the Gleissle mirror relations (Eqs. (49) and (50)). Finally, we note that increasing the damping function parameter a decreases the magnitude of the offset factor f (i.e. it increases the disparity between $\eta(\dot{\gamma})$ and $\eta^*(\omega)\big|_{\omega=\dot{\gamma}}$). From (33) and (34), we observe that the plateau value of f depends on the damping function parameter a in a power-law manner, and the low shear and high shear plateau scale as $f \sim a^{(\alpha-1)/2}$ and $f \sim a^{(\beta-1)/2}$ respectively. Renardy (1997) has shown that the Cox-Merz rule is valid for materials with a broad spectrum of relaxation times to within a constant factor. We have shown in this section that for complex multiscale materials with a relaxation modulus that can be well described by the Mittag-Leffler function, these constant factors can be quantified, and vary gradually with shear rate.

D. The Delaware-Rutgers rule for power-law Materials

For other classes of complex fluids such as concentrated suspensions which exhibit a yield stress, the Cox-Merz rule is known to fail. Instead, observations show that there exists a new relationship for yield-like materials that relates dynamic and steady-shear measurements, which Krieger (1992) has suggested be called the Rutgers-Delaware rule. Doraiswamy *et al.* (1991) have developed a nonlinear model for such materials, and the existence of this rule is rigorously proved. The rule states that dynamic measurements performed at frequency ω and shear strain amplitude γ_0 are equivalent to steady shear response performed at shear rate $\dot{\gamma}$ when $\gamma_0\omega = \dot{\gamma}$. The starting point of their model is an empirically introduced elastic Herschel-Bulkley type relationship for stress and strain. A critical strain parameter γ_c is

introduced, at which transition from elastic to inelastic behavior takes place. In what follows, we show that an appropriate choice of fractional constitutive model, along with a suitable damping function can give rise to not only a constitutive equation of Herschel-Bulkley type in steady shear but also a linear viscoelastic material response and agreement with the Rutgers-Delaware rule.

We consider a model of Fractional Kelvin-Voigt type (FKVM) with a Hookean spring in parallel with a springpot such that the total stress σ is given by

$$\sigma = \sigma^s + \sigma^{sp} \tag{54}$$

with σ^s being the stress in the spring and σ^{sp} the stress in the springpot. The elastic spring, however, is nonlinear and plastically yields at a critical strain $\gamma_c = \sigma_y/G$ so that the constitutive response is

$$\sigma^s = G\gamma^s, \ |\gamma^s| \leq \gamma_c \tag{55}$$

$$= G\gamma_c, \quad |\gamma^s| > \gamma_c \tag{56}$$

where G is the linear elastic modulus of the unyielded element and γ_c is a critical strain amplitude. We are now interested in determining the response of such a FKVM constitutive model under a steady shear rate $\dot{\gamma}$. To find the steady state response for the springpot, we use a K-BKZ approach as before, along with a damping function $h(\gamma)$ given by Tanner and Simmons (1967)

$$h(\gamma) = 1, \ \left|\gamma\right| \leq \gamma_c \tag{57}$$

$$= 0, \ \left|\gamma\right| > \gamma_c$$

The choice of this damping function is motivated by the fact that materials such as concentrated suspensions yield catastrophically (Dimitriou, Ewoldt, and McKinley (2013); Dzuy (1983)), and the elastic modulus of the material decreases sharply upon yield. We obtain

from Eq. (4) and Eq. (20) and expression for the stress in the springpot σ^{sp} that is given by

$$\sigma^{sp}(\dot{\gamma}) = \int_{-\infty}^{t} \frac{\mathbb{V}(-\alpha)}{\Gamma(1-\alpha)}(t-t')^{-\alpha-1} h(\gamma)\ \dot{\gamma}\ dt' \tag{58}$$

Making the variable substitution $\gamma = \dot{\gamma}(t-t')$ and noting that $\dot{\gamma}$ is constant, we obtain

$$\sigma^{sp}(\dot{\gamma}) = \dot{\gamma}^{\alpha} \int_{0}^{\infty} \frac{\mathbb{V}\alpha}{\Gamma(1-\alpha)} \gamma^{-\alpha} h(\gamma)\ d\gamma \tag{59}$$

and substituting for the damping function $h(\gamma)$ from Eq. (55) and solving the integral, we finally obtain

$$\sigma^{sp}(\dot{\gamma}) = \frac{\mathbb{V}\alpha}{\Gamma(2-\alpha)} \gamma_c^{1-\alpha} \dot{\gamma}^{\alpha} \tag{60}$$

The total stress $\sigma = \sigma^{s} + \sigma^{sp}$ in steady flow is now calculated using Eq. (56) and Eq. (60) as being

$$\sigma(\dot{\gamma}) = G\gamma_c + \frac{\mathbb{V}\alpha}{\Gamma(2-\alpha)} \gamma_c^{1-\alpha} \dot{\gamma}^{\alpha} \tag{61}$$

or equivalently the steady shear viscosity is given by

$$\eta(\dot{\gamma}) \equiv \frac{\sigma(\dot{\gamma})}{\dot{\gamma}} = \frac{G\gamma_c}{\dot{\gamma}} + \frac{\mathbb{V}\alpha}{\Gamma(2-\alpha)} \gamma_c^{1-\alpha} \dot{\gamma}^{\alpha-1} \tag{62}$$

Note that Eq. (62) is identical to the Herschel-Bulkley type stress-strain relationship proposed by Doraiswamy *et al.* (1991). It is immediately seen that at low shear rates

$$\eta(\dot{\gamma}) \approx \frac{G\gamma_c}{\dot{\gamma}} = \frac{\sigma_y}{\dot{\gamma}} \tag{63}$$

and at high shear rates

$$\eta(\dot{\gamma}) \approx \frac{\mathbb{V}\alpha\gamma_c^{1-\alpha}}{\Gamma(2-\alpha)} \dot{\gamma}^{\alpha-1} = K\dot{\gamma}^{\alpha-1} \tag{64}$$

The presence of the quasi-properties $\mathbb{V}$ and the power-law exponent α in the expression for the steady shear viscosity, which are independently determined from linear viscoelastic measurements, indicate that the linear and nonlinear rheology are interconnected through

the damping function and the parameter γ_c at which the material suddenly yields.

To derive the response of this elastoviscoplastic FKVM model in oscillatory flow, we assume that a deformation profile of the form $\gamma = \gamma_0 \sin(\omega t)$ is applied, in which γ_0 is the strain amplitude. Similar to Doraiswamy *et al.* (1991), we also assume that the material yields upon an infinitesimally small deformation (i.e. although we are interested in small amplitude oscillations and γ_0 is small, we assume the critical strain $\gamma_c \ll \gamma_0$.) This means that the nonlinear spring saturates and yields before the oscillating strain reaches its maximum amplitude.

Because we use a FKVM type model with elements in parallel, the stresses in each element are additive and hence

$$G'(\omega) = G'^{(s)}(\omega) + G'^{(sp)}(\omega) \tag{65}$$

$$G''(\omega) = G''^{(s)}(\omega) + G''^{(sp)}(\omega) \tag{66}$$

where the superscripts s and sp stand for spring and springpot respectively, as before. We know from linear viscoelasticity theory that (Macosko (1994))

$$G'^{(s)}(\omega) = \omega \int_0^\infty G(s) \sin(\omega s)\ ds \tag{67}$$

$$G''^{(s)}(\omega) = \omega \int_0^\infty G(s) \cos(\omega s)\ ds \tag{68}$$

Although the limits of the integral run from 0 to ∞, we have noted that the spring yields when the strain reaches γ_c in the first quarter cycle. This happens at time t_c given by

$$t_c = \frac{1}{\omega} \sin^{-1}\left(\frac{\gamma_c}{\gamma_0}\right) \tag{69}$$

Therefore, in Eqs. (67) and (68), $G(s) = G$ for $s \leq t_c$ and $G(s) = 0$ for $s > t_c$. Consequently, the limits of the integrals in Eq. (67) and Eq. (68) span from 0 to t_c. Evaluating these

integrals, we find that

$$G'^{(s)}(\omega) = G(1 - \cos\omega t_c) \approx \frac{G}{2}\left(\frac{\gamma_c}{\gamma_0}\right)^2 \tag{70}$$

$$G''^{(s)}(\omega) = G\sin\omega t_c = G\frac{\gamma_c}{\gamma_0} \tag{71}$$

In Eq. (70) we have used the fact that $\gamma_c \ll \gamma_0$ to approximate the cosine term using a Taylor series expansion.

To find $G'^{(sp)}(\omega)$ and $G''^{(sp)}(\omega)$, we use the K-BKZ equation with the Tanner-Simmons damping function given in Eq. (57). Therefore in this case Eq. (20) becomes

$$\sigma^{(sp)}(t) = \frac{\mathbb{V}(-\alpha)}{\Gamma(1-\alpha)}\int_{-\infty}^{t}(t-t')^{-(\alpha+1)}h[\gamma(t,t')][\gamma(t') - \gamma(t)]\; dt' \tag{72}$$

and making the variable transformation $u = t - t'$ we obtain

$$\sigma^{(sp)}(t) = \frac{\mathbb{V}\alpha}{\Gamma(1-\alpha)}\int_{0}^{\infty}u^{-(\alpha+1)}h[\gamma(t,t')][\gamma(t) - \gamma(t-u)]\; du \tag{73}$$

In Fig. 11 we show as a green line the absolute value of an applied deformation of the form $\gamma(t) = \gamma_0\sin(\omega t)$ for two complete cycles. The blue dashed line is a plot of $h(\gamma)$ defined in Eq. (57). Because $h(\gamma)$ depends only on the instantaneous value of the strain, whenever $\left|\gamma(t)\right| \leq \gamma_c$, $h(\gamma) = 1$, as seen in the figure. This means that any structural damage induced in the material at strains larger than γ_c is instantly undone when the strain drops below γ_c. This instantaneous recovery of material structure, however, is unphysical; in real materials there is typically a recovery time for the reversal of structural damage induced at large strains. In other words, any damage accumulated in the initial increasing portion of the sinusoidally oscillating strain will not be reversed instantaneously in the decreasing portion of the strain cycle. Wagner and Stephenson (1979) call this the irreversibility assumption, and show that for a LDPE melt, constitutive predictions of the rheological response in reversing flows are much improved by accounting for irreversibility. In line with this assumption, we modify our damping function and assume that there is *zero* recovery upon the strain reaching the critical value γ_c in the first cycle. Therefore, once $h(\gamma) = 0$, it remains zero for all subsequent times. This damping function is shown by the red circles in Fig. 11, and this

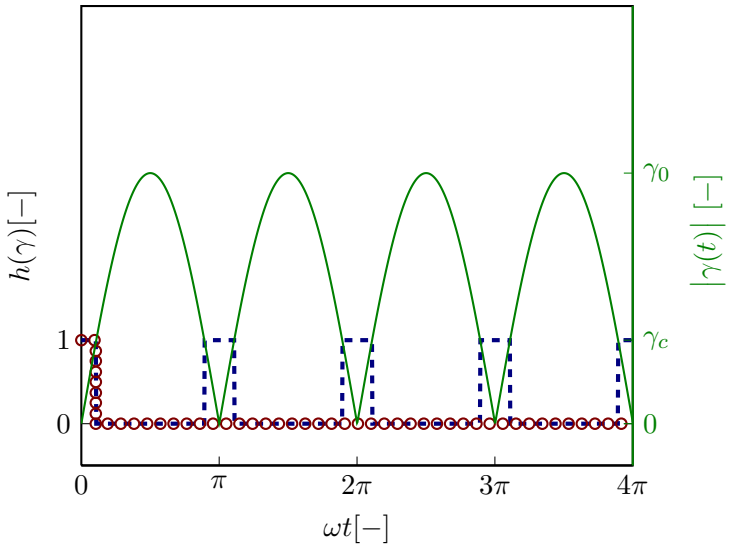

FIG. 11. The irreversibility assumption. The green line shows $\big|\gamma(t)\big| = \gamma_0\big|\sin\omega t\big|$. The blue dashed line is the damping function without the irreversibility assumption, and there is instant microstructural recovery of accumulated damage in the material when $\gamma < \gamma_c$. The red circles denote the damping function we use in (73), which accounts for irreversibility and assumes zero recovery after the strain first exceeds the critical strain γ_c.

is the function we use in our model, given by Eq. (73).

Substituting this damping function into Eq. (73) and noting that $\gamma(t) = \gamma_0 \sin\omega t$, we obtain

$$\sigma^{(sp)}(t) = \frac{\mathbb{V}\alpha\gamma_0}{\Gamma(1-\alpha)} \int_0^{u_c} u^{-(\alpha+1)}[\sin\omega t - (\sin\omega t\cos\omega u - \cos\omega t\sin\omega u)]\, du \tag{74}$$

in which u_c is given by

$$u_c = \frac{1}{\omega}\sin^{-1}\left(\frac{\gamma_c}{\gamma_0}\right) \approx \frac{1}{\omega}\frac{\gamma_c}{\gamma_0} \tag{75}$$

because $\gamma_c \ll \gamma_0$. Upon simplifying and separating the in-phase and out of phase components of the stress $\sigma^{(sp)}(t)$ with respect to the applied strain $\gamma(t)$ we obtain the storage and loss

moduli $G'^{(sp)}(\omega)$ and $G'^{(sp)}(\omega)$ respectively as

$$G'^{(sp)}(\omega) = \frac{\mathbb{V}\alpha}{\Gamma(1-\alpha)} \int_0^{u_c} u^{-(\alpha+1)}(1-\cos\omega u)\ du \tag{76}$$

$$G''^{(sp)}(\omega) = \frac{\mathbb{V}\alpha}{\Gamma(1-\alpha)} \int_0^{u_c} u^{-(\alpha+1)}\sin\omega u\ du \tag{77}$$

To analytically solve these integrals, we note that $0 \leq u \leq u_c \ll 1$, and we approximate $1 - \cos(\omega u) \approx (\omega u)^2/2$ and $\sin(\omega u) \approx \omega u$, from appropriate Taylor series expansions. Therefore we finally obtain

$$G'^{(sp)}(\omega) \approx \frac{\mathbb{V}\alpha\omega^\alpha}{2(2-\alpha)\Gamma(1-\alpha)} \left(\frac{\gamma_c}{\gamma_0}\right)^{2-\alpha} \tag{78}$$

$$G''^{(sp)}(\omega) \approx \frac{\mathbb{V}\alpha\omega^\alpha}{\Gamma(2-\alpha)} \left(\frac{\gamma_c}{\gamma_0}\right)^{1-\alpha} \tag{79}$$

We now use Eqs. (70), (71), (78) and (79) to find the overall elastic and loss moduli predicted by the model, and these are given by

$$G'(\omega) = \frac{G}{2}\left(\frac{\gamma_c}{\gamma_0}\right)^2 + \frac{\mathbb{V}\alpha\omega^\alpha}{2(2-\alpha)\Gamma(1-\alpha)} \left(\frac{\gamma_c}{\gamma_0}\right)^{2-\alpha} \tag{80}$$

$$G''(\omega) = G\frac{\gamma_c}{\gamma_0} + \frac{\mathbb{V}\alpha\omega^\alpha}{\Gamma(2-\alpha)} \left(\frac{\gamma_c}{\gamma_0}\right)^{1-\alpha} \tag{81}$$

with $\eta^*(\omega)$ given by Eq. (42) as before. From Eqs. (80) and (81), we see that

$$\frac{G'(\omega)}{G''(\omega)} \sim \frac{\gamma_c}{\gamma_0} \ll 1 \tag{82}$$

and therefore

$$\eta^*(\omega) = \frac{G''(\omega)\sqrt{1 + (G'(\omega)/G''(\omega))^2}}{\omega} \approx \frac{G''(\omega)}{\omega} \tag{83}$$

and consequently

$$\eta^*(\omega) = G\frac{\gamma_c}{\gamma_0\omega} + \frac{\mathbb{V}\alpha}{\Gamma(2-\alpha)}\gamma_c^{1-\alpha}(\gamma_0\omega)^{\alpha-1} \tag{84}$$

Comparing this result with Eq. (62), we find that

$$\eta^*(\omega) = \eta(\dot{\gamma})\big|_{\dot{\gamma}=\gamma_0\omega} \tag{85}$$

This result is identical to the Rutgers-Delaware rule. Krieger (1992) has noted in a brief correspondence that the Rutgers-Delaware rule is of a fundamentally different form to the Cox-Merz rule, and not merely an alternate form or extension of it. The Rutgers-Delaware rule applies to materials that are inherently nonlinear, and for which the period of oscillation is much shorter than the structural recovery time of the material. We incorporate both these properties of the material using our choice of Tanner-Simmons damping function, detailed in Fig. 11. The inherent nonlinearity is accounted for by assuming $\gamma_c/\gamma_0 \ll 1$; i.e. the elastoplastic material always yields and flows during the imposed oscillatory deformation. The long timescale typically associated with structural recovery in such materials is captured using our damping function by assuming zero recovery after the first yielding event, as shown in Fig. 11.

We have shown above that with an appropriate choice of a fractional constitutive model, not only can we develop a nonlinearly-elastic constitutive formulation of the familiar Herschel Bulkley model, but the resulting theoretical framework naturally gives rise to relationships such as the Rutgers-Delaware rule that relates oscillatory and steady shear rheology. We emphasize that the advantage of using a fractional constitutive model together with the K-BKZ framework is that we also obtain the linear viscoelastic response of multiscale yielding materials that exhibit a nonlinear rheological response of Herschel-Bulkley type; the linear and nonlinear properties are naturally related through the damping function.

In addition to the Herschel-Bulkley model discussed above, there are other empirical inelastic power-law models which can also be derived from first principles by an appropriate choice of fractional constitutive equation. We illustrate this process below by deriving the Cross and Carreau models starting with a Fractional Zener Model (FZM) and coupling it with a damping function using the K-BKZ framework.

E. Fractional Zener Model (FZM) and Carreau-Type Flow Curves

The FZM consists, in most general form, of a fractional Maxwell model branch in parallel with a single springpot (Schiessel *et al.* (1995)), resulting in three mechanical elements

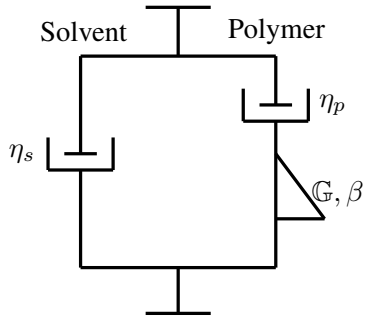

FIG. 12. A special case of the Fractional Zener Model (FZM) which we refer to as the Fractional Viscoelastic Cross Model (FVCM).

and six model parameters (a quasi-property and a power-law exponent for each springpot). Various forms of power-law response can be obtained from this model depending on the specific values of the power-law exponents and the corresponding quasi-properties of each of the springpots. In this paper, we will consider one special case of the FZM, as shown schematically in Fig. 12, in which two of the springpots are reduced to Newtonian dashpots. We show below that this four parameter model is well suited for describing concentrated polymer solutions and other shear-thinning multiscale systems.

The dashpot in the left-hand branch of the FZM has viscosity η_s and accounts for the background solvent viscosity. One of the springpots on the FMM branch (right-hand side of the FZM) is set to be a Newtonian dashpot with viscosity $\mathbb{V} = \eta_p$ and $\alpha = 1$. This dashpot accounts for the polymer contribution to the steady shear viscosity, and the shear viscosity is bounded by $\eta_0 = \eta_p + \eta_s$ as $\dot{\gamma} \to 0$. This FZM has a characteristic relaxation time given by $\tau = (\eta_p/\mathbb{G})^{1/(1-\beta)}$. The third springpot has a power-law exponent β and a quasi-property $\mathbb{G}$. Therefore, this model has a total of four parameters. We call this special case of the FZM the Fractional Viscoelastic Cross Model (FVCM) and we explain this choice of nomenclature below.

Following Schiessel *et al.* (1995), the constitutive equation of the FVCM can be written as

$$\sigma(t) + \frac{\eta_p}{\mathbb{G}} \frac{d^{1-\beta}}{dt^{1-\beta}} \sigma(t) = (\eta_p + \eta_s) \frac{d\gamma(t)}{dt} + \frac{\eta_p \eta_s}{\mathbb{G}} \frac{d^{2-\beta}\gamma(t)}{dt^{2-\beta}} \tag{86}$$

Using the Laplace and Fourier transform techniques already outlined in this article (Pod-

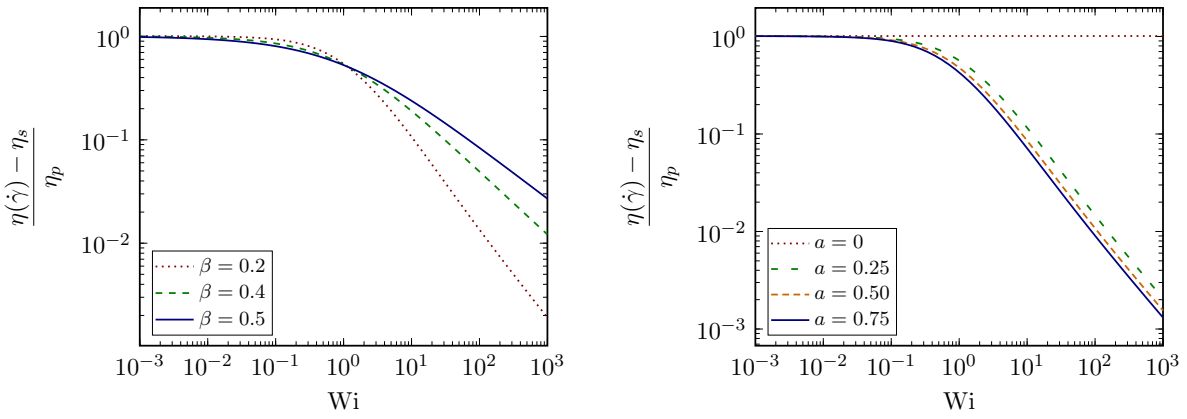

FIG. 13. Simulations of the viscosity predicted by the FVCM model plotted in dimensionaless form as a function of the Weissenberg number $\mathrm{Wi} = \tau\dot\gamma$. (a) Effect of varying the value of the springpot exponent β, which controls the slope of the shear-thinning region. (b) Effect of varying the damping function parameter a. For $a = 0$, no shear-thinning is observed.

lubny (1999)), the linear viscometric functions may be determined as follows:

$$G'(\omega) = \frac{\eta_p^2 \mathbb{G}\omega^{\beta+2}\cos(\pi\beta/2)}{(\eta_p\omega)^2 + (\mathbb{G}\omega^\beta)^2 + 2\eta_p\mathbb{G}\omega^{\beta+1}\sin(\pi\beta/2)} \tag{87}$$

$$G''(\omega) = \eta_s\omega + \frac{\mathbb{G}^2\eta_p\omega^{2\beta+1} + \eta_p^2\mathbb{G}\omega^{\beta+2}\sin(\pi\beta/2)}{(\eta_p\omega)^2 + (\mathbb{G}\omega^\beta)^2 + 2\eta_p\mathbb{G}\omega^{\beta+1}\sin(\pi\beta/2)} \tag{88}$$

$$G(t) = \eta_s\delta(t) + \mathbb{G}t^{-\beta}E_{1-\beta,1-\beta}\left(-\frac{\mathbb{G}}{\eta_p}t^{1-\beta}\right) \tag{89}$$

Because we have an expression for the relaxation modulus $G(t)$ we can use this in the K-BKZ framework as before (Eq. (18)) to compute the model predictions in large straining deformations. To evaluate the integral we need to specify the form of the damping function. Here we take the same simple form as Eq. (24) which adequately describes many systems and introduces one additional model parameter.

We present simulations of the steady shear viscosity predicted by the FVCM in Fig. 13. The values of η_s and η_p were chosen to be $\eta_s = 1$ Pa s and $\eta_p = 100$ Pa s. We choose to plot the predictions on dimensionless axes, with the steady shear viscosity $\eta(\dot\gamma)$ suitably scaled by η_p and η_s and the x axis is a Weissenberg number $\mathrm{Wi} = \tau\dot\gamma$, with τ being the characteristic

relaxation time given above. Fig. 13(a) shows the effect of changing the exponent β of the springpot, holding all other parameters constant. Increasing β decreases the slope of the shear-thinning region; in fact, because the shear-thinning region is controlled by the Maxwell arm of the FZM (the solvent term dictates the high shear rate viscosity plateau η_s), Eq. (34) is applicable and $\eta(\dot{\gamma}) \sim \dot{\gamma}^{\beta-1}$. We also show the effect of changing the strain damping parameter a in Fig. 13b. We observe that for $a = 0$, the damping function $h(\gamma) = 1$, and there is no shear-thinning because there is no microstructural damage accumulated in the material upon imposing large strains. For all non-zero values of a, shear-thinning is observed; as a is increased, it can be seen that at the same value of Weissenberg number Wi, the scaled viscosity is lower as expected. In this manner, the damping parameter a simply offsets each predicted curve from the next, when all other parameters are held constant.

When we consider the role of the five model parameters in this form of the FVCM, we find that the model has all the capabilities of the Cross model (Macosko (1994)) which proposes the following expression to capture the flow curves of polymer melts:

$$\eta(\dot{\gamma}) = \eta_s + \frac{\eta_p}{1 + (\dot{\gamma}/\dot{\gamma}^*)^{(1-n)}} \tag{90}$$

where $\eta(\dot{\gamma})$ is the steady shear viscosity. The parameters η_p and η_s control the zero shear and infinite shear plateau viscosities respectively, n dictates the slope of the power-law region between the two plateau regions and $\dot{\gamma}^*$ is a characteristic shear rate that determines the point of transition between the zero-shear plateau and the asymptotic power-law region. In Fig. 14 we show as a solid line the predicted steady shear viscosity $\eta(\dot{\gamma})$ obtained for the FVCM. The dashed line in the figure is the prediction of the Cross model. The model parameters used to obtain these simulations are given in the figure caption, and it is clear that the agreement between the FVCM and the Cross model is excellent.

The advantage of using the FVCM over the Cross model is three-fold: first, our approach also enables the determination of the linear viscoelastic material functions such as $G'(\omega)$ and $G''(\omega)$ (Eqs. (87) and (88) respectively) for materials that exhibit a flow curve that is captured by the Cross model. The inelastic Cross model does not have a linear viscoelastic limit at all. For example, if the shear rate $\dot{\gamma}$ were stepped up from $\dot{\gamma}_1$ to $\dot{\gamma}_2 > \dot{\gamma}_1$, the shear stress in the Cross model responds instantaneously. Second, the linear viscoelastic parameters play a role in nonlinear behavior and their relative contribution is weighted by

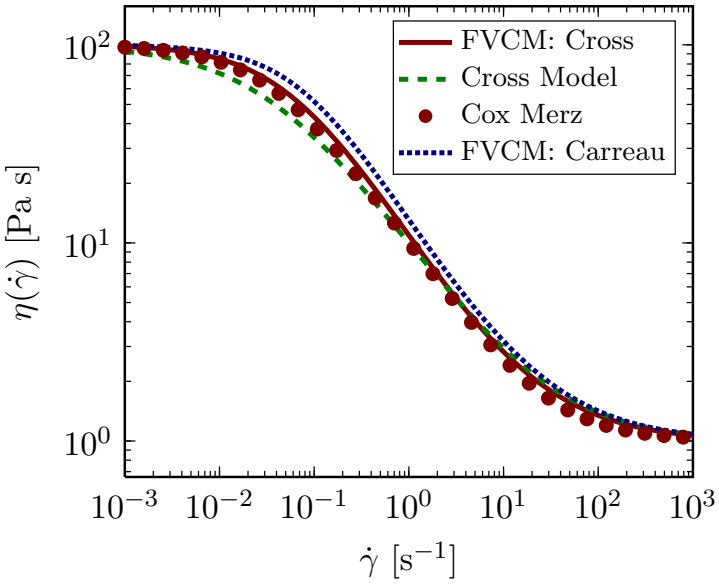

FIG. 14. Simulations of the the steady shear viscosity $\eta(\dot{\gamma})$ as a function of shear rate $\dot{\gamma}$ obtained from the FVCM model. For all curves, $\eta_p = 100$ Pa s and $\eta_s = 1$ Pa s. The FCVM (Cross) prediction was obtained using a damping function of the form $h(\gamma) = 1/(1+0.1\gamma^2)$ and a springpot with $\beta = 0.3$ and $\mathbb{G} = 10$ Pa s^β, and $\tau = (\eta_p/\mathbb{G})^{1/(1-\beta)} = 26.83$ s. To generate the Cross model simulation, the same values of $(\dot{\gamma}^*)^{-1} = 26.83$ s and $n = 0.3$ were chosen.

the damping function. We illustrate this point in Fig. 14 by showing the magnitude of the complex viscosity $|\eta^*(\omega)|$ at $\omega = \dot{\gamma}$, i.e., the prediction of the steady shear viscosity obtained from the application of the Cox-Merz rule (Eq. (41)) to the FVCM. Here too, we see that the magnitude of shear-thinning obtained from the linear viscoelastic properties agrees closely with the full nonlinear prediction as well as with the empirical Cross model. We also note in passing that the small offset between $\eta(\dot{\gamma})$ and $\eta^*(\omega)\big|_{\omega=\dot{\gamma}}$ can be quantified in terms of the damping function parameter a, as discussed previously. The third advantage of our fractional constitutive modeling approach to the Cross model is that the FVCM model also yields a prediction of the first normal stress coefficient $\Psi_1(\dot{\gamma})$ for materials such as concentrated polymer solutions that exhibit a Cross-like flow curve under steady shearing flow.

To generate the simulations of the FVCM in Fig. 14, note that we chose a damping function of the form $h(\gamma) = 1/(1 + a\gamma^2)$. In their review, Rolón-Garrido and Wagner (2009) discuss more complicated forms of the damping function. Conceivably, depending on the microstructural properties of the material, the form of the damping function could be different from the one we have chosen above. We show as a dotted line in Fig. 14 the

simulation of the steady shear viscosity $\eta(\dot{\gamma})$ obtained from Eq. (18) with the relaxation kernel given by Eq. (89) and a damping function of the form $h(\gamma) = \frac{1}{[1+(0.1\gamma^2)^3]^{1/3}}$. We observe that the transition from the zero shear viscosity plateau to the power-law shear-thinning region is now 'sharper', displaying behavior of the kind exhibited by the empirical Carreau model (Bird (1976); Bird, Armstrong, and Hassager (1987)). Hence, by controlling the damping function, we can reproduce a wide variety of steady flow curves (as commonly observed experimentally); these four linear viscoelastic parameters in the model remain unchanged and are determined from independent linear deformation histories such as SAOS.

V. CONCLUSIONS

There is a wealth of rheological data available in the literature on complex fluids that exhibit broad power-law–like behavior in their linear viscoelastic material properties. It has been shown in previous studies that fractional constitutive equations provide an excellent framework to quantitatively describe the linear rheological properties of multiscale materials. However, there was no mechanism for extending these models to nonlinear deformations. Using the concept of quasi-properties (Blair, Veinoglou, and Caffyn (1947b)), it is possible to compactly describe the linear rheology of power-law materials using an appropriate choice of fractional constitutive model. These models can be visualized as consisting of springs, dashpots and springpots in series or parallel. The resulting constitutive equations of these models are linear ODEs and can also be written in terms of linear convolution integrals with a relaxation modulus that is of Mittag-Leffler form. We have extended these linear viscoelastic models to make predictions of the nonlinear behavior of power-law materials using the K-BKZ framework. To evaluate the resulting integrals, we are required to determine the appropriate form of the material's damping function, for which we use a series of step strain experiments with increasing strain amplitude. This introduces just one additional model parameter, and results in a nonlinear integral equation given by Eq. (18). We use this model to make accurate predictions of both $\eta(\dot{\gamma})$ and $\Psi_1(\dot{\gamma})$ for Xanthan gum solutions and provide analytical approximations for both material functions.

Evaluating empirical rules such as the Cox-Merz relationship and the Gleissle mirror relations using this constitutive framework show that a shift factor exists, and that $\eta^*(\omega)\big|_{\omega=\dot{\gamma}} > \eta(\dot{\gamma})$. This is because the small amplitude deformations upon which these empirical rules

are based on do not account for the structural damage that is accumulated during a nonlinear deformation. Using our integral formulation, we quantify this shift factor (or offset) in terms of the linear viscoelastic as well as damping function parameters. In the limit of an exponential relaxation kernel of Maxwell-Debye form the offset is zero, but systematically increases for relaxation kernels of Mittag-Leffler form that more accurately capture the broad relaxation dynamics of complex materials such as Xanthan gum.

We also address a semi-empirical relationship that is fundamentally different from the Cox-Merz rule, but also relates steady shear and oscillatory experiments, known as the Rutgers-Delaware rule (Doraiswamy *et al.* (1991)). This rule applies to viscoelastoplastic materials such as concentrated suspensions exhibiting yield-like behavior beyond a critical strain. Starting with a Fractional Kelvin-Voigt representation we derive from first principles a viscoelastic generalization of the elastic Herschel-Bulkley equation, which correctly follows the Rutgers-Delaware rule. Finally, we have also shown how to derive a nonlinear viscoelastic model to quantify the nonlinear rheology of shear-thinning viscoelastic materials such as concentrated polymer solutions exhibiting Cross or Carreau-type behavior in steady shear flow.

In this manuscript, we have presented a framework that helps translate between the linear and nonlinear rheology of power-law multiscale materials. There are only two components that need to be determined within this framework: the fractional relaxation dynamics (specifically the memory kernel which describes the linear viscoelastic response), and the strain-dependent damping function. The extension of the fractional constitutive framework to the Cross or Carreau model detailed here opens up the possibility of accurately describing the rheological response of a large class of complex fluids in a general manner, using only a few model parameters. The resulting constitutive models provide a compact but accurate description of the linear and nonlinear viscoelastic properties of complex liquids and soft solids which should be useful for quantitative materials diagnostics, and quality control comparisons as well as for computational simulations.

APPENDIX A: HIGHER ORDER ANALYTICAL SOLUTION FOR $\eta(\dot{\gamma})$ AND $\Psi_1(\dot{\gamma})$

In the main text of this manuscript, we provide analytical expressions for $\eta(\dot{\gamma})$ and $\Psi_1(\dot{\gamma})$ (Eqs. (32) and (37) respectively). However, the solution presented is the lowest order term

of a more general higher order solution. For most experimental values of the exponents α and β, including for the fluids discussed in the main manuscript, a single term expansion is fine. But for $\alpha \to 1$ and/or $\beta \to 0$, higher order descriptions are needed.In this appendix we provide the derivation of the full analytical solution. However for the particular values of $\alpha = 1$ and $\beta = 0$, the Mittag-Leffler kernel reduces to an exponential, and hence does not have a power-law asymptote at long times. In this case, the integral must be solved explicitly with an exponential relaxation kernel. For all other values of $0 < \beta < \alpha < 1$, the analysis below holds.

We begin with the expression for the steady shear viscosity $\eta(\dot{\gamma})$ given by Eq. (25) as follows:

$$\eta(\dot{\gamma}) = -\mathbb{G} \int_0^\infty u^{-\beta} E_{\alpha-\beta,-\beta}\left(-\frac{\mathbb{G}}{\mathbb{V}} u^{\alpha-\beta}\right) \cdot \frac{1}{1+a(\dot{\gamma}u)^2}\, du \tag{91}$$

Note that in Eq. (25) we set the damping function constant $a = 0.3$ on account of this being the appropriate experimentally measured value for our Xanthan gum solutions, but in Eq. (91) we keep it general. Setting $\gamma = \dot{\gamma}u$, we obtain

$$\eta(\dot{\gamma}) = -\mathbb{G}\dot{\gamma}^{\beta-1} \int_0^\infty \frac{\gamma^{-\beta}}{1+a\gamma^2} E_{\alpha-\beta,-\beta}\left(-\frac{\mathbb{G}}{\mathbb{V}}\dot{\gamma}^{\beta-\alpha}\gamma^{\alpha-\beta}\right)\, d\gamma \tag{92}$$

As before, we split the integral with limits that range from 0 to ∞ into two different integrals as follows:

$$\begin{aligned}\eta(\dot{\gamma}) = -\,\mathbb{G}\dot{\gamma}^{\beta-1} \Bigg[&\int_0^{\gamma^*} \frac{\gamma^{-\beta}}{1+a\gamma^2} \sum_{k=1}^{\infty} \frac{\left(-\frac{\mathbb{G}}{\mathbb{V}}\dot{\gamma}^{\beta-\alpha}\gamma^{\alpha-\beta}\right)^{k-1}}{\Gamma((k-1)(\alpha-\beta)-\beta)}\, d\gamma \\ &+ \int_{\gamma^*}^{\infty} -\frac{\gamma^{-\beta}}{1+a\gamma^2} \sum_{k=1}^{\infty} \frac{\left(-\frac{\mathbb{G}}{\mathbb{V}}\dot{\gamma}^{\beta-\alpha}\gamma^{\alpha-\beta}\right)^{-k}}{\Gamma(-k(\alpha-\beta)-\beta)}\, d\gamma \Bigg]\end{aligned} \tag{93}$$

in which $\gamma^* = (\mathbb{V}/\mathbb{G})^{\alpha-\beta}\dot{\gamma} = \tau\dot{\gamma}$. The decomposition exploits the fact that the Mittag-Leffler function has well defined asymptotes for both small and large arguments, and has

the following expansions (Podlubny (1999))

$$E_{a,b}(z) = \sum_{k=1}^{N} \frac{z^{k-1}}{\Gamma(a(k-1)+b)} + \mathcal{O}\left(z^{N+1}\right),\ z \ll 1 \tag{94}$$

$$E_{a,b}(z) = -\sum_{k=1}^{N} \frac{z^{-k}}{\Gamma(b-ak)} + \mathcal{O}\left(z^{-(N+1)}\right),\ z \gg 1 \tag{95}$$

The Mittag-Leffler function smoothly transitions between its small argument power-law ($\sim z^0$) to its large argument power-law ($\sim z^{-1}$). By separating the integrals into two domains, we assume that the Mittag-Leffler function is piecewise continuous, and transitions from the power-law asymptote for $z \ll 1$ to the asymptote for $z \gg 1$ at the discrete point $\gamma = \gamma^*$.

We can solve for the integrals in Eq. (93) in terms of hypergeometric function defined in Eq. (31) and we obtain

$$\begin{aligned}\eta(\dot{\gamma}) = \sum_{k=1}^{N} \Bigg[&-\mathbb{G}\left(-\frac{\mathbb{G}}{\mathbb{V}}\right)^{k-1} \frac{\dot{\gamma}^{-p_k}}{\Gamma(p_k-1)} \frac{(\gamma^*)^{p_k}}{p_k} \times {}_2F_1\left(1, \frac{p_k}{2}, 1+\frac{p_k}{2}; -a(\gamma^*)^2\right) \\ &+ \\ &\mathbb{G}\left(-\frac{\mathbb{G}}{\mathbb{V}}\right)^{-k} \frac{\dot{\gamma}^{q_k-2}}{\Gamma(-q_k+1)} \frac{(\gamma^*)^{-q_k}}{aq_k} \times {}_2F_1\left(1, \frac{q_k}{2}, 1+\frac{q_k}{2}; \frac{-1}{a(\gamma^*)^2}\right)\Bigg]\end{aligned} \tag{96}$$

in which we have introduced the parameters

$$p_k = \alpha(k-1) - k\beta + 1 \tag{97}$$

$$q_k = \alpha k - (k-1)\beta + 1 \tag{98}$$

for ease of notation, we obtain

An analytical expression for the first normal stress coefficient $\Psi_1(\dot{\gamma})$, given by (36), can

be derived in an identical fashion, and we obtain

$$\Psi_1(\dot{\gamma}) = \sum_{k=1}^{N} \left[-\mathbb{G} \left(-\frac{\mathbb{G}}{\mathbb{V}} \right)^{k-1} \frac{\dot{\gamma}^{-p_k}}{\Gamma(p_k - 1)} \frac{(\gamma^*)^{p_k+1}}{p_k + 1} \times {}_2F_1 \left(1, \frac{p_k + 1}{2}, \frac{p_k + 3}{2}; -a(\gamma^*)^2 \right) \right.$$

$$+$$

$$\left. \mathbb{G} \left(-\frac{\mathbb{G}}{\mathbb{V}} \right)^{-k} \frac{\dot{\gamma}^{q_k-2}}{\Gamma(-q_k + 1)} \frac{(\gamma^*)^{1-q_k}}{a(q_k - 1)} \times {}_2F_1 \left(1, \frac{q_k - 1}{2}, \frac{q_k + 1}{2}; \frac{-1}{a(\gamma^*)^2} \right) \right] \quad (99)$$

Eq. (96) and (99) reduce to Eqs. (32) and (37), respectively, by retaining only the lowest order term, *i.e.* the $k = 1$ term and neglecting all higher order terms.

We note that Eq. (95) is strictly valid only in the limit of $z \gg 1$. However, for the purposes of our analytical approximation, we apply this asymptotic limit for $z \geq 1$ (cf. the second integral in Eq. (93); the limits of the argument of the Mittag-Leffler function range from 1 to ∞). In this second integral, as the value of k is increased, the term $1/\Gamma(-\beta - k(\alpha - \beta))$ begins to increase rapidly in magnitude and alternate in sign. This is easily seen by plotting the value of $1/\Gamma(x)$ for $x \leq 0$ (not shown here). Therefore, we in fact obtain poorer approximations for higher orders, beyond a certain value of k. Note that this counter-intuitive result would not have arisen if we had used a larger value of the lower limit in the second integral in Eq. (93), say $\gamma^* \to 10\gamma^*$, because the z^{-k} term, being large, would damp put these oscillations in the Gamma function. In this case, we could find the approximate solution up to large k, without diminishing accuracy.

However, we note that in practice, we rarely require large k; to check the accuracy and convergence of our approximation, we compared the exact numerical solution to Eq. (92) with the approximate solution given in Eq. (93) with various randomly generated values of $0 < \beta < \alpha < 1$ and $\mathbb{V}$, $\mathbb{G}$. We find that in all cases, we require at most $k = 3$ to get very close agreement between the approximate result and the exact numerical solution, and the $1/\Gamma(-\beta - k(\alpha - \beta))$ is well behaved.

APPENDIX B: CREEP RECOVERY

Single Springpot

The constitutive equation for a single springpot is given by

$$\sigma(t) = \mathbb{V}\frac{d^\alpha \gamma(t)}{dt^\alpha} \tag{100}$$

where $\sigma(t)$ and $\gamma(t)$ are the stress and the strain, respectively, in the element. Let us assume that the creep phase of the experiment is performed until time t_0. We are interested in the recovery phase of the experiment for all times $t > t_0$. In this phase, the applied stress $\sigma(t)$ is given by

$$\sigma(t) = \sigma_0(H(t) - H(t - t_0)) \tag{101}$$

in which $H(t)$ is the Heaviside step function given by $H(t) = 1$ for $t \geq 0$ and $H(t) = 0$ for $t < 0$, and σ_0 is the step in stress. Substituting equation (100) into equation (101) we have

$$\sigma_0(H(t) - H(t - t_0)) = \mathbb{V}\frac{d^\alpha \gamma(t)}{dt^\alpha} \tag{102}$$

Taking the Laplace transform of the equation (keeping in mind that $t > t_0$) we have

$$\sigma_0 \left(\frac{1 - e^{-st_0}}{s}\right) = \mathbb{V}s^\alpha \tilde{\gamma}(s) \tag{103}$$

where $\tilde{\gamma}(s)$ is the Laplace transformed strain. Therefore

$$\frac{\sigma_0}{\mathbb{V}} \left(\frac{1}{s^{\alpha+1}} - \frac{e^{-st_0}}{s^{\alpha+1}}\right) = \tilde{\gamma}(s) \tag{104}$$

and taking the inverse Laplace transform, we finally have

$$\gamma(t) = \frac{\sigma_0}{\mathbb{V}} \left(\frac{t^\alpha}{\Gamma(\alpha+1)} - \frac{(t-t_0)^\alpha}{\Gamma(\alpha+1)}\right) \tag{105}$$

In Fig. 15, we show an example of the creep compliance $J(t) = \gamma(t)/\sigma_0$ for a power-law material, followed by its behavior in the recovery phase. The specific model parameters chosen to generate this plot are given in the caption. The green line depicts the material

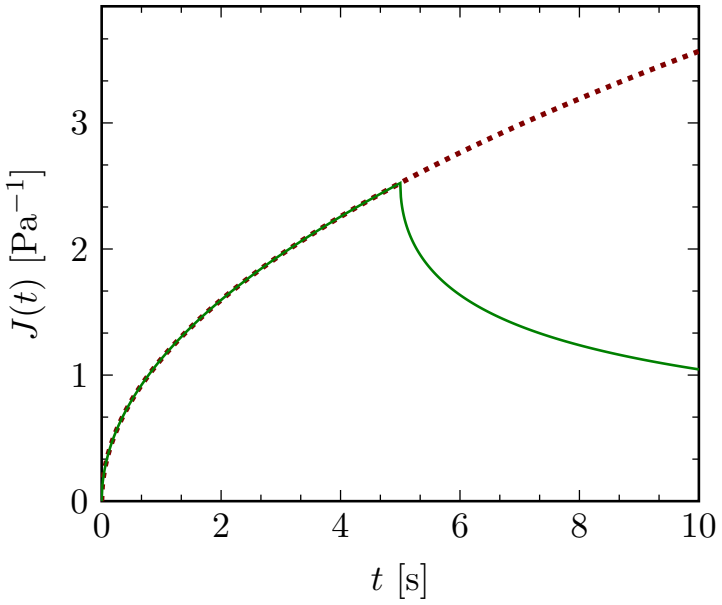

FIG. 15. Example of a creep experiment during flow as well as recovery. The model parameters chosen are $\alpha = 0.5$, $\mathbb{V} = 1$ Pa s$^{0.5}$ and $t_0 = 5$ s.

response for the entire creep experiment, including the recovery phase (i.e. the combined response of both terms in parenthesis in Eq. 105). The red dotted line is the response of the first term alone, which is identical to the creep response before the stress is removed.

We now examine the long time behavior of the above expression; we rewrite the expression as

$$\gamma(t) = \frac{1}{\Gamma(\alpha+1)} \frac{\sigma_0 t^\alpha}{\mathbb{V}} \left[1 - \left(1 - \frac{t_0}{t}\right)^\alpha\right] \tag{106}$$

For long times, $t_0/t \ll 1$, and using the Binomial theorem we have to leading order

$$\gamma(t) \approx \frac{\sigma_0}{\mathbb{V}\Gamma(\alpha+1)} t^\alpha \left[1 - \left(1 - \frac{\alpha t_0}{t}\right)\right] \tag{107}$$

$$\Rightarrow \gamma(t) \approx \frac{\sigma_0 t_0^\alpha}{\mathbb{V}\Gamma(\alpha)} \left(\frac{t}{t_0}\right)^{\alpha-1} \tag{108}$$

We therefore observe that the long time strain recovery for a single springpot is a power-law function of time.

Fractional Maxwell Model

In the FMM, the two springpots are in series and consequently the strains are additive. We can therefore simply add the strain recoveries of the two individual springpots to arrive at the full expression of the recovery. This expression is given by

$$\gamma(t) = \sigma_0 \left(\frac{t^\alpha - (t-t_0)^\alpha}{\mathbb{V}\Gamma(\alpha+1)} + \frac{t^\beta - (t-t_0)^\beta}{\mathbb{G}\Gamma(\beta+1)} \right) \tag{109}$$

We can now use a similar argument as shown above to find the long time asymptotic behavior of this expression, and we have for $t/t_0 \ll 1$

$$\gamma(t) \approx \frac{\sigma_0 t_0}{\mathbb{V}\Gamma(\alpha)} t^{\alpha-1} + \frac{\sigma_0 t_0}{\mathbb{G}\Gamma(\beta)} t^{\beta-1} \tag{110}$$

This expression can be simplified further. For large enough times, $t^{\alpha-1} > t^{\beta-1}$ and hence to leading order the strain during recovery is given by

$$\gamma(t) \approx \frac{\sigma_0 t_0^\alpha}{\mathbb{V}\Gamma(\alpha)} \left(\frac{t}{t_0} \right)^{\alpha-1} \tag{111}$$

REFERENCES

Abramowitz, M. and Stegun, I. A., *Handbook of Mathematical Functions* (U.S. National Bureau of Standards, Washington, 1964).

Bagley, R. L. and Torvik, P. J., "A theoretical basis for the application of fractional calculus to viscoelasticity," Journal of Rheology **27**, 201 (1983a).

Bagley, R. L. and Torvik, P. J., "Fractional calculus - A different approach to the analysis of viscoelastically damped structures," AIAA Journal **21**, 741–748 (1983b).

Bird, R. B., "Useful non-Newtonian models," Annual Review of Fluid Mechanics **8**, 13–34 (1976).

Bird, R. B., Armstrong, R. C., and Hassager, O., *Dynamics of Polymeric Liquids*, 2nd ed. (John Wiley & Sons, 1987).

Blair, G. W. S., Veinoglou, B. C., and Caffyn, J. E., "Limitations of the Newtonian time scale in relation to non-equilibrium rheological states and a theory of quasi-properties,"

Proceedings of the Royal Society A: Mathematical, Physical and Engineering Sciences **189**, 69–87 (1947a).

Blair, G. W. S., Veinoglou, B. C., and Caffyn, J. E., "Limitations of the Newtonian Time Scale in Relation to Non-Equilibrium Rheological States and a Theory of Quasi-Properties," Proceedings of the Royal Society A: Mathematical, Physical and Engineering Sciences **189**, 69–87 (1947b).

Booij, H. C. and Leblans, P., "Nonlinear viscoelasticity and the Cox-Merz relations for polymeric fluids," Journal of Polymer Science: Polymer Physics Edition **21**, 1703–1711 (1983).

Caputo, M., "Linear models of dissipation whose Q is almost frequency independent - II," Geophysical Journal International **13**, 529–539 (1967).

Cox, W. P. and Merz, E. H., "Correlation of Dynamic and Steady Flow Viscosities," Journal of Polymer Science **28**, 619–622 (1958).

Craiem, D. and Magin, R. L., "Fractional order models of viscoelasticity as an alternative in the analysis of red blood cell (RBC) membrane mechanics." Physical Biology **7**, 13001 (2010).

Cuvelier, G. and Launay, B., "Concentration regimes in xanthan gum solutions deduced from flow and viscoelastic properties," Carbohydrate Polymers **6**, 321–333 (1986).

Dealy, J. M., "Weissenberg and Deborah numbers-their definition and use," Rheology Bulletin **79**, 14–18 (2010).

Dealy, J. M. and Wissbrun, K. F., *Melt Rheology and its Role in Plastics Processing: Theory and Applications.* (Van Nostrand Reinhold, New York, 1990).

Dimitriou, C. J., Ewoldt, R. H., and McKinley, G. H., "Describing and prescribing the constitutive response of yield stress fluids using large amplitude oscillatory shear stress (LAOStress)," Journal of Rheology **57**, 27 (2013).

Djordjević, V. D., Jarić, J., Fabry, B., Fredberg, J. J., and Stamenović, D., "Fractional derivatives embody essential features of cell rheological behavior," Annals of Biomedical Engineering **31**, 692–699 (2003).

Doraiswamy, D., Mujumdar, A. N., Tsao, I., Beris, A. N., Danforth, S. C., and Metzner, A. B., "The Cox-Merz rule extended: A rheological model for concentrated suspensions and other materials with a yield stress," Journal of Rheology **35**, 647–685 (1991).

Dzuy, N. Q., "Yield stress measurement for concentrated suspensions," Journal of Rheology **27**, 321–349 (1983).

English, R. J., Raghavan, S. R., Jenkins, R. D., and Khan, S. A., "Associative polymers bearing n-alkyl hydrophobes: Rheological evidence for microgel-like behavior," Journal of Rheology **43**, 1175–1194 (1999).

Ewoldt, R. H. and McKinley, G. H., "Creep ringing in rheometry or how to deal with oft-discarded data in step stress tests!" Rheology Bulletin **76**, 4–6 (2007).

Fabry, B., Maksym, G., Butler, J., Glogauer, M., Navajas, D., and Fredberg, J., "Scaling the Microrheology of Living Cells," Physical Review Letters **87**, 148102 (2001).

Friedrich, C., "Relaxation functions of rheological constitutive equations with fractional derivatives: thermodynamical constraints," in *Rheological Modelling: Thermodynamical and Statistical Approaches* (Springer-Verlag, 1991) pp. 321–330.

Friedrich, C., "Rheological material functions for associating comb-shaped or H-shaped polymers A fractional calculus approach," Philosophical Magazine Letters **66**, 287–292 (1992).

Friedrich, C. and Braun, H., "Generalized Cole-Cole behavior and its rheologial relevance," Rheologica Acta **322**, 309–322 (1992).

Friedrich, C., Schiessel, H., and Blumen, A., "Constitutive Behavior Modeling and Fractional Derivatives," in *Advances in the Flow and Rheology of Non-Newtonian Fluids*, edited by D. A. Siginer, D. De Kee, and R. P. Chhabra (1999) pp. 429–266.

Gallegos, C., Franco, J. M., and Partal, P., "Rheology of food dispersions," Rheology reviews , 19–65 (2004).

Glockle, W. G. and Nonnenmacher, T. F., "Fractional integral operators and Fox functions in the theory of viscoelasticity," Macromolecules **24**, 6426–6434 (1991).

Goh, K. K. T., Matia-Merino, L., Hall, C. E., Moughan, P. J., and Singh, H., "Complex rheological properties of a water-soluble extract from the fronds of the black tree fern, Cyathea medullaris." Biomacromolecules **8**, 3414–3421 (2007).

Guskey, S. M. and Winter, H. H., "Transient shear behavior of a thermotropic liquid crystalline polymer in the nematic state," Journal of Rheology **35**, 1191–1207 (1991).

Heymans, N. and Podlubny, I., "Physical interpretation of initial conditions for fractional differential equations with Riemann-Liouville fractional derivatives," Rheologica Acta **45**, 765–771 (2005).

Jaishankar, A. and McKinley, G. H., "Power-law rheology in the bulk and at the interface: quasi-properties and fractional constitutive equations," Proceedings of the Royal Society A: Mathematical, Physical and Engineering Sciences **469**, 2012.0284 (2013).

Ketz, R. J., Prud'homme, R. K., and Graessley, W. W., "Rheology of concentrated microgel solutions," Rheologica Acta **27**, 531–539 (1988).

Khan, S. A., Schnepper, C. A., and Armstrong, R. C., "Foam rheology: III. Measurement of shear flow properties," Journal of Rheology **32**, 69–92 (1988).

Koeller, R. C., "Applications of fractional calculus to the theory of viscoelasticity," Journal of Applied Mechanics **51**, 299–307 (1984).

Krieger, I., "Correspondence : Comments on a manuscript Doraiswamy et al." Journal of Rheology **36**, 215–217 (1992).

Krishnamoorti, R. and Giannelis, E. P., "Rheology of end-tethered polymer layered silicate nanocomposites," Macromolecules **30**, 4097–4102 (1997).

Lapasin, R. and Pricl, S., *Rheology of Industrial Polysaccharides: Theory and Applications* (Blackie Academic and Professional, Glasgow, 1995).

Larson, R. G., "Constitutive relationships for polymeric materials with power-law distributions of relaxation times," Rheologica Acta **24**, 327–334 (1985).

Larson, R. G., *Constitutive Equations for Polymer Melts and Solutions* (Butterworths, Boston, 1988).

Laun, H. M., "Prediction of elastic strains of polymer melts in shear and elongation," Journal of Rheology **30**, 459–501 (1986).

Leblans, P. J. R., Sampers, J., and Booij, H. C., "The mirror relations and nonlinear viscoelasticity of polymer melts," Rheologica Acta **24**, 152–158 (1985).

Lion, A., "On the thermodynamics of fractional damping elements," Continuum Mechanics and Thermodynamics **9**, 83–96 (1997).

Ma, L. and Barbosa-Canovas, G. V., "Simulating viscoelastic properties of selected food gums and gum mixtures using a fractional derivative model," Journal of Texture Studies **27**, 307–325 (1996).

Macosko, C. W., *Rheology Principles, Measurements and Applications* (Wiley-VCH, New York, 1994).

Mainardi, F., *Fractional Calculus and Waves in Linear Viscoelasticity: an Introduction to Mathematical Models.* (World Scientific Press, 2010).

Markovitz, H., "Boltzmann and the beginnings of linear viscoelasticity," Transactions of the Society of Rheology **21**, 381–398 (1977).

Mason, T., "Estimating the viscoelastic moduli of complex fluids using the generalized Stokes-Einstein equation," Rheologica Acta **39**, 371–378 (2000).

Mason, T. G. and Weitz, D. A., "Linear viscoelasticity of colloidal hard sphere suspensions near the glass transition." Physical Review Letters **75**, 2770–2773 (1995).

Metzler, R., Barkai, E., and Klafter, J., "Anomalous diffusion and relaxation close to thermal equilibrium: a fractional fokker-planck equation approach," Physical review letters **82**, 3563–3567 (1999).

Metzler, R. and Klafter, J., "The random walk's guide to anomalous diffusion: A fractional dynamics approach." Physics Reports **339**, 1–77 (2000).

Metzler, R. and Klafter, J., "From stretched exponential to inverse power-law: fractional dynamics, Cole-Cole relaxation processes, and beyond," Journal of Non-Crystalline Solids **305**, 81–87 (2002).

Metzler, R., Schick, W., Kilian, H.-G., and Nonnenmacher, T. F., "Relaxation in filled polymers: A fractional calculus approach," The Journal of Chemical Physics **103**, 7180 (1995).

Miller, K. S. and Ross, B., *An Introduction to the Fractional Calculus and Fractional Differential Equations* (John Wiley & Sons, Inc., 1993).

Muthukumar, M., "Dynamics of polymeric fractals," The Journal of Chemical Physics **83**, 3161 (1985).

Ng, T. S. and Mckinley, G. H., "Power law gels at finite strains : The nonlinear rheology of gluten gels," Journal of Rheology **52**, 417–449 (2008).

Nonnenmacher, T. F., "Fractional relaxation equations for viscoelasticity and related phenomena," Rheological Modelling: Thermodynamical and Statistical Approaches , 309–320 (1991).

Oertel, R. and Kulicke, W. M., "Viscoelastic properties of liquid crystals of aqueous biopolymer solutions," Rheologica Acta **30**, 140–150 (1991).

Oldham, K. B. and Spanier, J., *The Fractional Calculus - Theory and Applications of Differentiation and Integration to Arbitrary Order* (Academic Press, New York, 1974).

Podlubny, I., *Fractional Differential Equations* (Academic Press, San-Diego, 1999).

Rees, D. A. and Welsh, E. J., "Secondary and Tertiary Structure of Polysaccharides in Solutions and Gels," Angewandte Chemie **16**, 214–224 (1977).

Renardy, M., "Qualitative correlation between viscometric and linear viscoelastic functions," Journal of non-Newtonian Fluid Mechanics **68**, 133–135 (1997).

Rich, J. P., McKinley, G. H., and Doyle, P. S., "Size dependence of microprobe dynamics during gelation of a discotic colloidal clay," Journal of Rheology **55**, 273–299 (2011).

Rochefort, W. E. and Middleman, S., "Rheology of xanthan gum: salt, temperature, and strain effects in oscillatory and steady shear experiments," Journal of Rheology **31**, 337–369 (1987).

Rolón-Garrido, V. H. and Wagner, M. H., "The damping function in rheology," Rheologica Acta **48**, 245–284 (2009).

Ross-Murphy, S. B., "Structure-property relationships in food biopolymer gels and solutions," Journal of Rheology **39**, 1451–1463 (1995).

Ross-Murphy, S. B., Morris, V. J., and Morris, E. R., "Molecular viscoelasticity of xanthan polysaccharide," Faraday Symposia of the Chemical Society **18**, 115–129 (1983).

Sanchez, C., Renard, D., Robert, P., Schmitt, C., and Lefebvre, J., "Structure and rheological properties of acacia gum dispersions," Food Hydrocolloids **16**, 257–267 (2002).

Schiessel, H., Metzler, R., Blumen, A., and Nonnenmacher, T., "Generalized viscoelastic models: their fractional equations with solutions," Journal of Physics A: Mathematical and General **28**, 6567–6584 (1995).

Sharma, R. and Cherayil, B. J., "Polymer melt dynamics: Microscopic roots of fractional viscoelasticity," Physical Review E **81**, 021804 (2010).

Sharma, V. and McKinley, G. H., "An intriguing empirical rule for computing the first normal stress difference from steady shear viscosity data for concentrated polymer solutions and melts," Rheologica Acta **51**, 487–495 (2012).

Sokolov, I. M., Klafter, J., and Blumen, A., "Fractional Kinetics," Physics Today **55**, 48 (2002a).

Sokolov, I. M., Klafter, J., and Blumen, A., "Fractional kinetics," Physics Today **55**, 48 (2002b).

Sollich, P., "Rheological constitutive equation for a model of soft glassy materials," Physical Review E **58**, 738–759 (1998).

Soskey, P. R. and Winter, H. H., "Large step shear strain experiments with parallel-disk rotational rheometers," Journal of Rheology **28**, 625 (1984).

Surguladze, T., "On certain applications of fractional calculus to viscoelasticity," Journal of Mathematical Sciences **112**, 4517–4557 (2002).

Tako, M., "Molecular origin for rheological characteristics of xanthan gum," in *ACS Symposium Series Vol. 489* (1992) pp. 268–281.

Tanner, R. I. and Simmons, J. M., "Combined simple and sinusoidal shearing in elastic liquids," Chemical Engineering Science **22**, 1803–1815 (1967).

Torvik, P. J. and Bagley, R. L., "On the appearance of the fractional derivative in the behavior of real materials," Journal of Applied Mechanics **51**, 294–298 (1984).

Valério, D., Trujillo, J. J., Rivero, M., Machado, J. A. T., and Baleanu, D., "Fractional calculus: A survey of useful formulas," The European Physical Journal Special Topics **222**, 1827–1846 (2013).

Venkataraman, S. K. and Winter, H. H., "Finite shear strain behavior of a crosslinking polydimethylsiloxane near its gel point," Rheologica Acta **29**, 423–432 (1990).

Wagner, M., Raible, T., and Meissner, J., "Tensile stress overshoot in uniaxial extension of a LDPE melt," Rheologica Acta **18**, 427–428 (1979).

Wagner, M. H. and Stephenson, S. E., "The irreversibility assumption of network disentanglement in flowing polymer melts and its effects on elastic recoil predictions," Journal of Rheology **23**, 489–504 (1979).

Whitcomb, P. J. and Macosko, C., "Rheology of Xanthan Gum," Journal of Rheology **22**, 493–505 (1978).

Winter, H. H. and Mours, M., "Rheology of polymers near liquid-solid transitions," in *Advances in Polymer Science, Vol. 134* (Springer-Verlag, 1997) pp. 165–234.

Yalpani, M., Hall, L. D., Tung, M. A., and Brooks, D. E., "Unusual rheology of a branched, water-soluble chitsan derivative," Nature **302**, 812–814 (1983).

Yang, P., Lam, Y. C., and Zhu, K.-Q., "Constitutive equation with fractional derivatives for the generalized UCM model," Journal of Non-Newtonian Fluid Mechanics **165**, 88–97 (2010).